2021-08-06

Simultaneous electrochemical determination of caffeine and theophylline in human serum, tea, and tablet samples using poly(ACP2CuIH) modified glassy carbon electrode

: Wagnew, Asefa

Bahir Dar University

College of Science Postgraduate Program

Department of Chemistry

MSc Thesis on

Simultaneous electrochemical determination of caffeine and theophylline in human serum, tea, and tablet samples using poly(ACP_2CuIH) modified glassy carbon electrode

By: Asefa Wagnew Mulu

Advisor: Professor Meareg Amare

July, 2021

Bahir Dar, Ethiopia

BAHIR DAR UNIVERSITY

COLLEGE OF SCIENCE POSTGRADUATE PROGRAM

DEPARTMENT OF CHEMISTRY

MSc THESIS ON

SIMULTANEOUS ELECTROCHEMICAL DETERMINATION OF CAFFEINE AND THEOPHYLLINE IN HUMAN SERUM, TEA, AND TABLET SAMPLES USING POLY(ACP_2CuIH) MODIFIED GLASSY CARBON ELECTRODE

A THESIS SUBMITTED TO COLLEGE OF SCIENCE POSTGRADUATE PROGRAM IN PARTIAL FULFILMENT TO THE REQUIREMENTS FOR THE DEGREE OF MASTER OF SCIENCE IN ANALYTICAL CHEMISTRY.

BY: ASEFA WAGNEW MULU

ADVISOR: PROFESSOR MEAREG AMARE

JULY, 2021

 BAHIR DAR, ETHIOPIA

APPROVAL SHEET

BAHIR DAR UNIVERSITY

POSTGRADUATE STUDIES

I, the undersigned declare that this thesis work which entitles as **"SIMULTANEOUS ELECTROCHEMICAL DETERMINATION OF CAFFEINE AND THEOPHYLLINE IN HUMAN SERUM, TEA, AND TABLET SAMPLES USING POLY(ACP_2CuIH) MODIFIED GLASSY CARBON ELECTRODE"** prepared under my supervision and guidance by Asefa Wagnew Mulu and recommended that the thesis be accepted as it fulfills the requirements for the degree of master of science in analytical chemistry.

Professor Meareg Amare	_____	_____
Name of Advisor	Signature	Date

A member of the Board of Examiners of MSc thesis open defense examination, we certify that we have read and evaluated the thesis prepared by Asefa Wagnew Mulu and we have examined the candidate. We approved that the thesis is accepted as a complement to the thesis requirement for the degree of Master of Science in Analytical Chemistry.

Molla Tefera (PhD)	_____	_____
Name of external examiner	Signature	Date
Belete Assefa (PhD)	_____	_____
Name of internal examiner I	Signature	Date
Tesfaye Shiferaw (PhD)	_____	_____
Name of internal examiner II	Signature	Date

DECLARATION

I, the undersigned, declare that this thesis, entitled **"SIMULTANEOUS ELECTROCHEMICAL DETERMINATION OF CAFFEINE AND THEOPHYLLINE IN HUMAN SERUM, TEA, AND TABLET SAMPLES USING POLY(ACP_2CuIH) MODIFIED GLASSY CARBON ELECTRODE"** is my original work under the supervision of Professor Meareg Amare that it has not been submitted to any other institution anywhere for the award of academic degree, diploma or certificate, that I followed all ethical and technical principles of scholarship in the data analysis and preparation of this report. I have acknowledged all referred materials used in this work.

Place of submission: Bahir Dar University, College of Science, Department of Chemistry

Submitted by:

Asefa Wagnew Mulu	_____	_____
Name of student	Signature	Date

ACKNOWLEDGEMENT

First and foremost I would like to thank and praise the almighty God for giving me good health, encouragement, and good spirit to complete this work.

I would like to express my sincere gratitude to my Advisor; Profesor Meareg Amare for his unwavering guidance, advice, and invaluable comments throughout the work of this thesis besides the ideas, suggestions, and selecting title up to for the accomplishment of this work. I appreciate and thank him for his positive and humanity when I need him any time and welcome in his office with his brotherly advice and encouragement, so thank you very much.

I would like to thank Doctor Ataklit Abebe (PhD), for providing the complex monomer and giving ideas for the complex character.

I would like to thank PhD student, Mr. Adane Kassa, for his cordial collaboration that enabled me to conduct all of the experiments in Electroanalytical Chemistry Research Laboratory Data Analysis.

I would like my family to give me moral and economical support, especially my mother Amarech Kelkay, my father Wagnew Mulu, and also my brother Yitayew Wagnew and my sister Meseret Wagnew.

I extend my special thanks to all my friends and colleagues, especially Mr. Merko Tarekegn, and Mr. Mesfin Mersha, they helped me morally and sensitively.

I would like to show my gratitude to MSc students of analytical chemistry particularly Amha Debalkie and Asnakech Mebrie for their friendship, ideas and continuous support in carrying out this study.

Finally, I would like to acknowledge Bahir Dar University, Science College, and the Department of Chemistry for allowing me to conduct this research work.

TABLE OF CONTENT

Contents page

ACKNOWLEDGEMENT i
TABLE OF CONTENT ii
LIST OF FIGURES iv
LIST OF TABLES vi
ABBREVIATION vii
1 INTRODUCTION 1
1.1 Background 1
1.2 Statement of the Problem 3
1.3 Objectives of the Study 4
1.3.1 General Objective 4
1.3.2 Specific Objectives 4
1.4 Significance of the Study 4
2 LITERATURE REVIEW 5
2.1 Xanthine 5
2.1.1 Caffeine 5
2.1.2 Theophylline 6
2.2 Electrochemical Techniques 8
2.2.1 Voltammetry 8
2.2.2 Types of Working Electrodes 18
3 MATERIALS AND METHODS 20
3.1 Chemicals and Apparatus 20
3.2 Procedure 20
3.2.1 Electrode Modification 20
3.2.2 Electrochemical Measurements 21
3.2.3 Preparation of Standard Stock and Working Solutions 21
3.2.4 Preparation of Real Samples 21
4 RESULTS AND DISCUSSION 23
4.1 Fabrication and Characterization of Poly(ACP_2CuIH)/GCE 23
4.2 Characterization of Poly(ACP_2CuIH)/GCE 24
4.2.1 Characterization by Cyclic Voltammetry 24
4.2.2 Characterization by EIS 24
4.3 Cyclic Voltammetric Study of TP and CAF at Poly(ACP_2CuIH)/GCE 26
4.3.1 Electrochemical Behavior of TP and CAF at Poly(ACP_2CuIH)/GCE 26
4.3.2 Effect of Scan Rate on the Peak Current and Peak Potential of CAF and TP 27
4.3.3 Effect of pH on Peak Current and Peak Potential of TP and CAF 30
4.4 SWV Investigation of TP and CAF at Poly(ACP_2CuIH)/GCE 31
4.4.1 Optimization of Square Wave Voltammetric Parameters 32
4.4.2 Calibration Curves of TP and CAF 33

4.5 Simultaneous Determination of CAF and TP in Real Samples....37
4.5.1 Tea Samples....37
4.5.2 Tablet Samples....38
4.5.3 Human Blood Serum Sample....39
4.6 Method Validation....40
4.6.1 Spike Recovery Study....40
4.6.2 Interference Study....43
4.7 Stability of the Poly(ACP_2CuIH)/GCE....47
4.8 Comparison of Present Method with Previously Reported Methods....48
5 CONCLUSION AND RECOMMENDATION....49
5.1 Conclusion....49
5.2 Recommendation....50
6 REFERENCES....51

LIST OF FIGURES

Figure 1.1: Structure of N-methyl derivative compounds.....1
Figure 2.1: (A) Potential-excitation signal and voltammogram for LSV, (B) Potential–time excitation signal and Voltammogram with key parameters in a CV experiment.....11
Figure 2.2: (A) Potential-excitation Signals and voltammograms for DPV, (B) SWV: potential–time waveform and SWV of a reversible reaction (A. forward, B. reverse and C. net current).....17
Figure 4.1: Cyclic voltammograms of GCE in pH 7.0 PBS containing 1.0 mM poly(ACP_2CuIH)/GCE scanned between -1.2 and +1.8 V for 15 cycles at a scan rate of 100 mV s^{-1}. Inset: (A) CVs of (a) first cycle and (b) fifteenth cycle, (B) CVs of (2) bare GCE, and (1) stabilized poly(ACP_2CuIH)/GCE in monomer free 0.5 M H_2SO_4 scanned between -0.8 and 0.8 V at scan rate of 100 mV s^{-1}.....23
Figure 4.2: CVs of unmodified (a) and modified (b) GCEs in pH 7.0 PBS containing 10 mM $[Fe(CN)_6]^{3-/4-}$ and 0.1 M KCl at scan rate of 100 mV s^{-1}.....24
Figure 4.3: Nyquist plots for (a) bare GCE and (b) poly(ACP_2CuIH)/GCE in pH 7.0 PBS containing 10.0 mM $[Fe(CN)_6]^{3-/4-}$ and 0.1 M KCl at frequency range: 0.01–100,000 Hz, applied potential: +0.23 V, and amplitude: 0.01 V.....25
Figure 4.4: CVs of bare GCE (a, c) and poly(ACP_2CuIH)/GCE (b, d) in 0.1 M ABS pH 5.0 containing no (a, b) and 1.0 mM CAF and TP (c, d) at scan rate of 100 V s^{-1}. Inset: corrected for blank CVs of (A) bare GCE, and (B) poly(ACP_2CuIH)/GCE. 27
Figure 4.5: (A) CVs of poly(ACP_2CuIH)/GCE in pH 5.0 ABS containing equi-molar (1.0 mM) mixture of TP and CAF at various scan rates (a–l: 10, 20, 40, 60, 80, 100, 125, 150, 175, 200, 250 and 300 mV s^{-1}, respectively), plot of (B) Ip vs. ν, (C) Ip vs. $\nu^{1/2}$, and (D) log (Ip) vs. log (ν). 29
Figure 4.6: Plot of Ep_a vs. lnν/ V s^{-1} of poly(ACP_2CuIH)/GCE in pH 5.0 ABS containing equi-molar (1.0 mM) mixture of TP and CAF at various scan rates (a–l: 10, 20, 40, 60, 80, 100, 125, 150, 175, 200, 250 and 300 mV s^{-1}, respectively). 30
Figure 4.7: (A) Representative CVs of poly(ACP_2CuIH)/GCE in ABS of various pHs (a–g: 3.0, 3.5, 4.0, 4.5, 5.0, 5.5, and 6.0, respectively) containing equi-molar (1.0 mM) mixture of TP and CAF, plot of mean ($\bar{x} \pm$ %RSD) (B) Ep and (C) Ip vs. pH in the entire pH range.....31
Figure 4.8: Corrected for blank SWVs of (a) bare GCE and (b) poly(ACP_2CuIH)/GCE in pH 4.5 ABS containing 1.0 mM TP and CAF at step potential: 6 mV, amplitude: 35 mV, and frequency: 20 Hz.....32
Figure 4.9: SWVs of poly(ACP_2CuIH)/GCE in pH 4.5 ABS containing 1.0 mM mixture of CAF and TP, (A) at various step potential (a–e: 2, 4, 6, 8, and 10 mV, respectively), amplitude of 25 mV, and frequency of 15 Hz. Inset: Plot of Ip vs. step potential, (B) at various square wave amplitudes (a–h: 10, 20, 25, 30, 35, 40, 45 and 50 mV, respectively), step potential of 6 mV, and frequency of 15 Hz. Inset: Plot of Ip vs. amplitude, (C) at step potential of 6 mV, amplitude of 35 mV, and various frequencies (a–d: 10, 15, 20, and 25 Hz, respectively). Inset: Plot of Ip vs. frequency.....33

Figure 4.10: Background subtracted SWVs of poly (ACP_2CuIH)/GCE in pH 4.5 ABS containing different concentrations of (A) CAF (a–i: 1.0, 5.0, 10.0, 20.0, 40.0, 80.0, 120.0, 160.0, and 200.0 µM, respectively) and 60.0 µM TP, and (B) TP (a-i: 1.0, 5.0, 10.0, 20.0, 40.0, 80.0, 120.0, 160.0, and 200.0 µM, respectively) and 60.0 µM CAF. Insets: Plot of peak current vs. concentration, at step potential: 6 mV, amplitude: 35 mV, and frequency: 20 Hz. 35
Figure 4.11: (A) Corrected for background SWVs of varying equi-molar mixtures of TP and CAF in pH 4.5 ABS (a–i: 1.0, 5.0, 10.0, 20.0, 40.0, 80.0, 120.0, 160.0 and 200.0 µM, respectively) at poly(ACP_2CuIH)/GCE. (B) Plot of the Ipa of TP (a) and CAF (b) (%RSD as error bar) vs. concentration, at step potential: 6 mV, amplitude: 35 mV, and frequency: 20 Hz.....36
Figure 4.12: SWVs of poly(ACP_2CuIH)/GCE in pH 4.5 ABS containing (A) Addis tea, (B) Black lion tea, and (C) Wush wush tea at the optimized SWV parameters.....37
Figure 4.13: Corrected for blank SWVs of poly(ACP_2CuIH)/GCE in pH 4.5 PBS containing A) Panadol tablet brand, and B) Theodrine tablet brand at the optimized SWV parameters. 38
Figure 4.14: Corrected for blank SWVs of human blood serum in pH 4.5 ABS spiked with equi-molar mixtures of TP and CAF (a–c: 0.0, 80.0 µM mixture, and 120.0 µM mix of TP + CAF, respectively) at poly(ACP_2CuIH)/GCE. 39
Figure 4.15: Corrected for blank SWVs of A) Black lion tea, B) Wush wush, and C) Addis tea samples all spiked with TP and CAF (a–c: real tea sample + 0.0 TP and CAF, a + 100.0 µM TP, and a + 100.0 µM + 100.0 µM CAF, respectively) at poly(ACP_2CuIH)/GCE.....41
Figure 4.16: Corrected for blank SWVs of poly(ACP_2CuIH)/GCE in pH 4.5 ABS containing (A) Panadol tablet brand spiked with TP and CAF (a–c: unspiked tablet sample, a + 80.0 µM TP, and a + 80.0 µM each mix of TP and CAF, respectively), and (B) Theodrine tablet brand spiked with TP and CAF (a–c: unspiked tablet sample, a + 80.0 µM CAF, and a + 80.0 µM each mix of TP and CAF, respectively). 43
Figure 4.17: Corrected for blank SWVs of poly(ACP_2CuIH)/GCE in pH 4.5 ABS containing Black lion tea spiked with 100.0 µM TP in the presence of various concentrations (a–e: 0.0, 50.0, 100.0, 150.0, and 200.0 µM, respectively) of A) Urea, B) Ephedrine, C) Paracetamol, and D) Sodium chloride. 44
Figure 4.18: Corrected for blank SWVs of poly(ACP_2CuIH)/GCE in pH 4.5 ABS containing a mix of Panadol tablet with nominal 80.0 µmol L^{-1} CAF and Theodrine tablet with nominal 80.0 µmol L^{-1} TP in the presence of A) Glucose, B) Ephedrine, C) Ascorbic Acid, and D) Paracetamol of various concentrations (a-e: tablet mix + 0.0, a + 40.0, a + 80.0, a + 120.0, and a + 160.0 µmol L^{-1}, respectively). 46
Figure 4.19: Five repetitive SWVs of poly(ACP_2CuIH)/GCE in pH 4.5 ABS containing a mixture of 1.0 M CAF and TP recorded in one day at an interval of two hrs.....48

LIST OF TABLES

Table 4.1 Summary of the calculated values of the RC- parameters: 26
Table 4.2 Summary of detected CAF and TP content in Panadol extra and Theodrine tablet samples using the developed method and percent detected as compared to the nominal value (n = 3). 39
Table 4.3 Simultaneous determination of TP and CAF in human blood serum samples spiked with an equi-molar mixture of TP and CAF standard (n= 3). 40
Table 4.4 Simultaneous determination of TP and CAF in Addis tea, Wush wush tea, and Black lion tea samples spiked with 100.0 μM TP and equi-molar mixture of 100.0 μM TP and CAF (n = 3). 42
Table 4.5 Summary of spike recovery results (mean±%RSD, n = 3) of TP and CAF in Theodrine and Panadol extra tablet samples. 43
Table 4.6 Summary of percentage interference recovery results of TP and CAF in Black tea sample spiked with 100.0 μM TP in the presence of selected potential interferents (Urea, Paracetamol, Ephedrine, and Sodium chloride) at their various levels. 45
Table 4.7 Summary of percentage interference recovery results of TP and CAF in tablet samples in the effect of potential interfering species on the simultaneous determination of 80.0 μM TP in Theodrine tablet and 80.0 μM CAF in Panadol extra tablet (n = 3).....47
Table 4.8 Comparison of the performance of the present method with previously reported methods in terms of selected parameters. 48

ABBREVIATION

Abbreviation	Definition
AA	Ascorbic Acid
ABS	Acetate Buffer Solution
CAF	Caffeine
CV	Cyclic Voltammetry
EIS	Electrochemical Impedance Spectroscopy
FTIR	Fourier Transform Infrared Spectroscopy
DPV	Differential Pulse Voltammetry
GCE	Glassy Carbon Electrode
HPLC	Higher Performance Liquid Chromatography
LoD	Limit Of Detection
LoQ	Limit Of Quantification
LSV	Linear Sweep Voltammetry
PBS	Phosphate Buffer Solution
Poly(ACP_2CuIH)/GCE	Poly(Aquachlorobis(1,10-Phenanthroline)cupper(II)iodidemonohydrate)
RSD	Relative Standard Deviation
SEM	Scanning Electron Microscopy
SPE	Solid-Phase Extraction
SWV	Square Wave Voltammetry
TB	Theobromine
TP	Theophylline
UV	Ultraviolet-Visible Spectroscopy
XRD	X-Ray Diffraction

ABSTRACT

*Cyclic voltammetric and electrochemical impedance spectroscopic results showed potentiodynamic deposition of a noble poly(aquachlorobis(1,10-phenanthroline)cupper(II)iodidemonohydrate) (poly(ACP_2CuIH)) polymer film on the surface of glassy carbon electrode. In contrast to the unmodified glassy carbon electrode, poly(ACP_2CuIH) film modified glassy carbon electrode (*poly(ACP_2CuIH)/GCE) *in a solution containing equi molar mixture of theophylline and caffeine revealed well separated oxidative peaks with much enhanced peak current and reduced over-potential showing the electrocatalytic property of the polymer film towards the oxidation of theophylline and caffeine. Poly(ACP_2CuIH)/GCE was used for square wave voltammetric simultaneous determination of theophylline and caffeine in various real samples including pharmaceutical tablets, tea, and human serum samples. Under optimized solution and square wave voltammetric parameters, oxidative peak current response of poly(ACP_2CuIH)/GCE showed a linear dependence on the concentration of caffeine and theophylline in a reasonably wide range of concentration. The method showed exactly the similar sensitivity towards simultaneous theophylline and caffeine as does for their separate detection. The current response of poly(ACP_2CuIH/GCE for simultaneous detection of theophylline and caffeine showed a linear dependence on the respective concentration in the range of 1–200.0 μM with a limit of detection of 8.92×10^{-9} M for theophylline, and 1.02×10^{-8} M for caffeine. The method was successfully used to detect theophylline and caffeine in tea (Black lion, Addis, and Wush wush), pharmaceutical tablet (Panadol extra and Theodrine), and human blood serum real samples with excellent recovery results of 97.0–102.0% and 95.4–96.8%, 99.0–101.0 and 98.9–100.0, and 100.0–101.4% and 98.9–99.3%, respectively. The accuracy, selectivity, stability, and reproducibility results validated the developed method for its applicability for simultaneous determination of theophylline and caffeine in complex matrix real samples including tablet formulation, tea, and human blood serum samples.*

Keywords*: Theophylline; Caffeine; Human blood serum; Modified electrode; Poly(aquachlorobis(1,10 – phenanthroline)cupper(II)iodidemonohydrate*

1 INTRODUCTION

1.1 Background

Caffeine (1, 3, 7-trimethylxanthine), theophylline (1, 3-dimethylxanthine), and theobromine (3, 7-dimethylxanthine) (Fig. 1.1) are natural methylxanthine purine bases which are known to act as anti-depressants, anti-therapeutic and anti-hyperuraemic agents [1]. Caffeine (CAF), theophylline (TP), and theobromine (TB) are N-methylxanthines that are naturally found in food products such as tea, coffee, cocoa beans, cola nuts, and mate leaves [1-3].

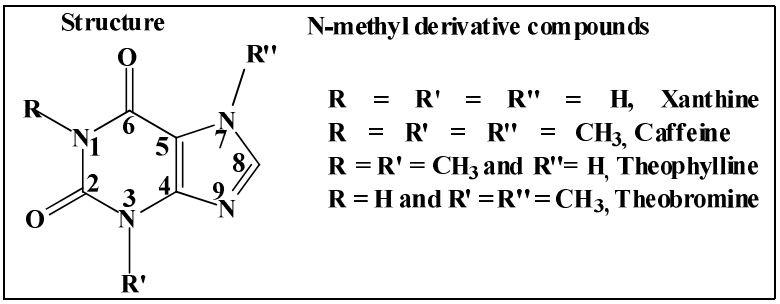

Figure 1.1: Structure of N-methyl derivative compounds

N-methylxanthine derivatives are alkaloids with distinctive bioactivity that received increasing attention in the food and pharmaceutical industries [4]. CAF stimulates the central nervous system and hence increases alertness, reduces sleep, improves short term memory, and increases the effectiveness of certain drugs [5]. Moderate CAF intake of 400 mg/day is not associated with adverse health effects; however, an overdose of CAF (> 400 mg/day) causes many undesired health effects such as irritability, hypertension and insomnia, loss of appetite, gastrointestinal complications, cardiovascular problems, and even death at dosages above 10 g/day [6, 7]. CAF is consumed daily in coffee, tea, cocoa, chocolate, energy drinks, and some drugs, therefore its monitoring and regulation is essential for regulatory authorities, the food industry, and health practitioners [7, 8]. Due to this, its use was regulated by the International Olympic Committee (positive controls for more than 12 mg/mL of urine) [9].

TP is widely employed as a bronchodilator drug in the management of several asthmatic conditions. The most accepted range of effective plasma TP concentrations in adults is between 5–20 μg mL^{-1}. While the levels below this range are usually non-therapeutic, higher levels may cause serious toxicity [10]. TP intoxication may manifest in headache, nausea, vomiting, increased acid secretion, gastroesophageal, reflux, heart-burn tachycardia, seizures,

insomnia, anorexia, central nervous system excitation, and even convulsions and cardiac arrhythmias at higher concentrations [10, 11]. Therefore, it is necessary to determine the concentrations of CAF and TP in real samples including pharmaceuticals, drinks, food, and human physiological liquids.

Different techniques have been reported for the detection of TP and CAF, including ion chromatography [4], high-performance liquid chromatography (HPLC) [3, 12, 13], electrospray ionization ion mobility spectrometry (ESI-IMS) [14], weak cation monolithic SPE-column [15] and spectrophotometry [16]. However, these techniques require expensive instruments, skilled operators, large sample volume, tedious sample pretreatment procedures, and long analysis time [6, 17]. Electrochemical detection is an alternative technique that has attracted attention due to its advantages including fast response time, low-cost instrument, simple, higher sensitivity, and faster operation than the conventional methods [6, 17, 18].

Recently, a few electrochemical sensors have been reported in literature for the individual determination of CAF [19-21] and TP [22-24] in real samples. Moreover, only limited electrochemical sensors using chemically modified electrodes including; novel poly(folic acid) [17], large mesoporous carbon/Nafion [25], non-enzymatic electrochemical sensor [26], poly(Alizarin Violet 3B) [27], and poly(L-aspartic acid)/functionalized multi-walled carbon nanotubes [28] have been reported on simultaneous determination of CAF and TP. However, simultaneous determination of TP and CAF is still faced with challenges. Firstly, TP and CAF have more positive oxidation potentials, which may lead to large background currents. Secondly, the oxidation products of the two compounds are adsorbed strongly on the electrode surface, the consequence of which lowering the method sensitivity and reproducibility [17, 25]. Thus, the development of an alternative method for simultaneous determination of TP and CAF with improved sensitivity, and reproducibility is still an area of interest.

This work presents a new voltammetric method for simultaneous determination of CAF and TP based on poly(aquachlorobis(1,10-phenanthroline)cupper(II)iodidemonohydrate) modified glassy carbon electrode (poly(ACP_2CuIH)/GCE) which to the best of our knowledge is only reported for determination of amoxicillin [29].

1.2 Statement of the Problem

Although moderate CAF intake to the level of 400 mg/day is not associated with adverse health effects, an overdose of CAF (> 400 mg/day) causes many undesired health effects such as irritability, hypertension and insomnia, loss of appetite, gastrointestinal complications, cardiovascular problems, and even death at dosages above 10 g/day. CAF is consumed daily in coffee, tea, cocoa, chocolate, energy drinks, and some drugs, therefore monitoring and regulating its level is essential for regulatory authorities, the food industry, and health practitioners. Due to this, its use was regulated by the International Olympic Committee (positive controls for more than 12 mg/mL of urine).

TP, which is taken as a bronchodilator drug in the management of several asthmatic conditions, is the most accepted range of effective plasma TP concentrations in adults (5–20 $\mu g\ mL^{-1}$). While the levels below this range are usually non-therapeutic, higher levels may cause serious toxicity. TP intoxication may manifested in headache, nausea, insomnia, anorexia, heart-burn tachycardia vomiting, increased acid secretion, gastroesophageal, reflux, seizures, central nervous system excitation, and even convulsions and cardiac arrhythmias.

The health effects associated with high doses of these alkaloids necessitates the development of a simple, sensitive, selective, cheap, and stable method for simultaneously monitoring their levels in real samples is crucial.

1.3 Objectives of the Study

1.3.1 General Objective

To develop a voltammetric method based on poly(ACP_2CuIH)/GCE for simultaneous determination of caffeine and theophylline in real samples including tablet, tea, and human blood serum samples.

1.3.2 Specific Objectives

- ✓ Evaluate the catalytic property of the poly(ACP_2CuIH)/GCE towards CAF and TP against the bare GCE.
- ✓ Optimize solution and method parameters for simultaneous determination of CAF and TP.
- ✓ Develop SWV method for simultaneous determination of CAF and TP based on poly(ACP_2CuIH)/GCE.
- ✓ Validate the developed method using selected validation parameters including linear dynamic range, method detection limit, accuracy (spike recovery), selectivity (interference recovery), and stability.
- ✓ Apply the developed method for the determination of CAF and TP in real samples including tablet, human blood serum, and tea samples.
- ✓ Compare the analytical performance of the developed method with literature reports.

1.4 Significance of the Study

The outcome of this study may be helpful for many stakeholders including researchers in the area, food factories, customers, health institutions, end-user patients, pharmaceutical factories, quality control, regulatory authorities, institutions like the International Olympic Committee, and professionals working on method development for the simultaneous determination of theophylline and caffeine.

2 LITERATURE REVIEW

2.1 Xanthine

Xanthine (3, 7-dihydro-purine-2,6-dione) is a purine base that can naturally be found in human body tissues and fluids as well as in plants and other organisms [30]. It is found in muscle tissue, liver spleen, pancreas, and other organs as well as in the urine [31]. Methylxanthines (methylated xanthines; Fig. 1.1 for chemical structure) are a unique class of drugs that are derived from the purine base xanthine [31]. Methylxanthines have different effects: reduce inflammation and immunity, reduce sleepiness, and increase alertness, but also stimulate the heart rate and contraction and dilate the bronchi [30]. They are a group of naturally occurring agents present as caffeine, theophylline, and theobromine. Naturally, they occur in substances found in coffee, tea, chocolate, cocoa drinks, and related foodstuffs [31]. They are purine alkaloids and have multiple pharmacological effects [32].

2.1.1 Caffeine

Caffeine (3,7-dihydro-1,3,7-trimethyl-1H-purine-2,6-dione) is an active natural alkaloid component, which is present with other trace purines that are primarily found in coffee, cola nuts, cocoa beans, tea leaves, yerba mate, guarana berries, other plant species [33]. CAF has been referred to as a purine alkaloid identified as early as 1875 by Medicus as 1, 3,7-trimethylxanthine [34], which closely resembles with important endogenous metabolites such as purines, xanthenes, and uric acid. Excessive CAF consumption may be detrimental and can lead to headaches, anxiety, stress, and an increased heart rate. Although some drugs contain CAF, due to the lack of substantiation of caffeine's negative effects, it is still used in the pharmacological preparation of painkillers [35].

2.1.1.1 Health Benefits of Caffeine

The suggested amount of CAF is normally 400 mg per day (equivalent to 4 to 5 cups of coffee) for healthy adults. High CAF consumption can also worsen pre existing health conditions, such as anxiety [8]. Research indicates that CAF may help to protect human brain cells, which lowers the risk of developing some diseases, (such as Parkinson's), regular cups of coffee may stimulate the gallbladder and reduce the risk of gallstones, it causes the blood vessels to constrict, which may help relieve some headache pain, reduces inflammation, and may help prevent certain heart related illnesses, treats migraine, relieves asthma attack,

increases the potency of analgesics and also used for weight loss and type 2 diabetes. Generally CAF, in moderate doses, can reduce fine motor coordination; increase alertness, nervousness, and headaches and cause insomnia and dizziness [19]. CAF intake may have some effects on sleep, mood, and blood pressure, so it is clinically used as a central nervous stimulant and has analgesic effects [32].

2.1.1.2 Adverse Effects of Caffeine

The occurrence of adverse effects of CAF consumption depends on the individual sensitivity to CAF and the level of daily consumption, such as caffeinated drinks. Acute adverse effects of CAF include nervousness, irritability, insomnia, nausea, headache, tremor, increased anxiety, cognitive disorders, arrhythmia, tachycardia, increased body temperature, elevated respiratory rate, gastrointestinal disorders, and reduction of myocardial blood flow. High repeated exposure over an extended period of time to CAF has been associated with a range of dysfunctions involving the gastrointestinal system, liver, renal system, musculature, and also with reduced fetal growth in pregnant women [36], vascular disease, depression, and heart disease, which can bring about cancer and even death [32]. The scientific literature report on CAF relative to possible cardiovascular effects; total cardiovascular disease, coronary heart disease, and acute myocardial infarction, arrhythmia, heart failure, sudden cardiac arrest, stroke, blood pressure, hypertension, heart Rate, and cerebral blood flow [7]

2.1.2 Theophylline

Theophylline (3, 7-dihydro-1, 3-dimethyl-1*H*-purine-2, 6-Dione) is a methylxanthine with a long history of use as an inexpensive bronchodilator. TP is still one of the most widely prescribed drugs for the treatment of asthma and chronic obstructive pulmonary disease (COPD) worldwide. TP occurs naturally in tea, from which it may be extracted. It was first synthesized chemically in 1895 and used initially as a diuretic. Its bronchodilator property was later identified, and it was introduced as a clinical treatment for asthma in 1922. Despite its widespread global use, TP has become a third-line treatment for asthma an add-on therapy in patients with poorly controlled diseases. TP has been supplanted for asthma therapy by inhaled β_2-adrenergic receptor agonists for bronchodilation and inhaled corticosteroids for anti-inflammatory effect. TP is used as an oral therapy (rapid or slow-release tablets) or as more soluble aminophylline, an ethylenediamine salt, which is suitable for oral and intravenous use [37].

TP, a member of xanthine based alkaloids, which relaxes smooth muscle and relieves bronchospasm, has a stimulant effect on respiration. The association of these drugs might produce a synergy effect in the therapy. TP has been marketed in combination with ephedrine in pharmaceutical formulations for being used in the symptomatic treatment of bronchial asthma and other bronchospastic conditions [38].

2.1.2.1 Health Benefits of Theophylline

TP is used to treat lung diseases such as anosmia, infant Apnea, asthma, and chronic obstructive pulmonary disease (COPD) (bronchitis, emphysema). It must be used regularly to prevent wheezing and shortness of breath. This medication belongs to a class of drugs known as xanthines or methylpurine drugs, which can dilate coronary arteries, relax bronchial smooth muscle, and stimulate the central nervous system, is mainly used for the treatment of bronchial asthma, emphysema, bronchitis, and cardiac dyspnea [32, 39].

2.1.2.2 Adverse Effects of Theophylline

Theophylline has a very narrow therapeutic window, and its interaction with various other drugs has led to the limitation of its use. The serum TP concentrations require monitoring directly to avoid toxicity as the adverse effects of TP are related to its plasma concentration and have been observed when plasma concentrations exceed 20 mg/L. Some patients have also experienced adverse effects at low plasma concentrations. The dose gradually increases until achieving therapeutic plasma concentrations. This approach reduces side effects. The most common side effects are nausea, vomiting, headache, increased stomach acid secretion, and gastroesophageal reflux, which could be due to phosphodiesterase (PDE) inhibition. Central nervous system symptoms (irritability, lightheadedness, and dizziness) can also occur in patients. In severe cases, seizures have also occurred. At high serum concentration of TP, adenosine A_{1A}-receptor antagonism could lead to convulsions and cardiac arrhythmias [37], diarrhea, which may result in permanent nerve damage and cardiac arrest [32].

2.2 Electrochemical Techniques

Electrochemical techniques are powerful and versatile analytical techniques that offer high sensitivity, accuracy, precision, and large linear dynamic range, with relatively low-cost instrumentation. After developing more sensitive pulse methods, the electroanalytical studies are more regularly used on industrial, environmental applications and on drug analysis in their dosage forms and especially in biological samples. However, electroanalytical techniques can easily solve many problems of pharmaceutical interest with a high degree of accuracy, precision, sensitivity, and selectivity. Some of the most useful electroanalytical techniques are based on the concept of continuously changing the applied potentials to the electrode-solution interface and the resulting measured current. Most of the chemical compounds were found to be electrochemically active [40].

2.2.1 Voltammetry

The term voltammetry refers to a class of electrochemical techniques, and it is used to designate the current-voltage measurement obtained at a given electrode, the current being proportional to the concentration of analyte in the sample [41]. Polarography is a special case of voltammetry referring to the current-voltage measurement acquired using dropping mercury electrodes with a constant flow of mercury drop. Czech chemist Jaroslav-Heyrovsky first introduced Polarography in 1922, for which he received the 1959 Nobel Prize in chemistry [42].

A Voltammetric cell usually is consisting of three electrode system immersed in a solution containing the analyte and supporting electrolyte;

a. The working electrode (Gold, Mercury, Platinum, Graphite and Various forms of carbon),

b. Counter or auxiliary electrode (platinum foil, coil...); which is a non-reactive high surface area electrode, commonly platinum gauze.

c. Reference electrode (calomel or Ag/AgCl electrode).

This relationship could be explained when potential (E) is applied to the working electrode and the resulting current (I) flowing through the electrochemical cell will be recorded. The applied potential could be changed or the resulting current will be recorded over a period of time (t) [42]. The potential applied to the working electrode serves as the driving force for the

reaction; it is controlled by the parameter that causes the chemical species present in the solution to be electrolyzed (reduced or oxidized) at the electrode surface.

The instrument, which monitors current-voltage curves (polarograph), was invented by Heyrovsky and Shikata. The resulting current-voltage plot is called voltammogram where current is displayed in the vertical axis and potential in the horizontal axis various.

Voltammetric techniques including cyclic voltammetry, and linear sweep voltammetry of the sweep techniques and square wave voltammetry, differential pulse voltammetry, and stripping voltammetry of the pulse techniques are among the widely reported techniques for the determination of pharmaceutical compounds [43].

2.2.1.1 Linear Sweep Voltammetry

Linear sweep voltammetry (LSV) involves monitoring the current as a function of applied potential when a regularly varying potential is applied to the working electrode. When scanning linearly across a series of potentials, the observed current is a function of potential and time (Fig. 2.1A). The potential limits can be applied depending on the reference electrode, the working electrode material, and the nature and composition of the supporting electrolyte. In LSV, the potential of the working is ramped from an initial potential to a final potential as shown in (Fig. 2.1A). The potential of the working electrode is changed linearly with time. The solution is unstirred and linear diffusion is maintained in this technique. The scan rate direction can be signed for showing the potential scan direction as negative for a cathodic sweep and positive for an anodic sweep. With this technique, the peak current is proportional to scan rate and large signals are obtained with very fast scans. The LSV method is a very useful electrochemical technique with most solid electrodes because rapid analysis times can be achieved with about a 10^{-6} M detection limit. The maximum current is called peak current and the corresponding potential is called peak potential. Peak potential gives the qualitative information of the investigated compound. Also, peak current or peak height gives the quantitative amount of the compounds [44].

2.2.1.2 Cyclic Voltammetry

Cyclic voltammeter (CV) is an electroanalytical technique reported in 1938 and described theoretically in 1948 by Randles and Sevcik. It has grown enormously in its popularity over the past few decades so much so that obtaining CV is often the first experiment performed by the electrochemist giving invaluable information as to the presence of electro active species

in solution. CV enables rapid observation of the redox behavior of an analyte over the entire potential range available. CV is an essential technique for initial electrochemical studies of new systems and has also proven very useful in obtaining mechanistic information about fairly complicated electrode reactions. Although CV is particularly useful in qualitative studies of electrode processes, it is less well suited for quantitative measurement of potentials or currents [45].

CV is a rapid voltage scan technique in which the direction of the voltage scan is reversed. While the applied potential at the working electrode in both forward and reverse directions the resulting current is recorded. The scan rate in the forward and reverse direction is normally the same. CV can be used in a single cycle or multicycle mode [46].

The measured parameters in CV are anodic and cathodic peak potential (Epa and Epc), anodic, and cathodic peak current (Ipa and Ipc), and the half peak potentials (Ep/2) at which the cathodic and anodic currents reach half of their peak value [46].

The analysis and methodology for the extraction of characteristic parameters obtained from cyclic voltammogram are shown in (Fig. 2.1B). A zero current line for the forward scan data has to be chosen (dashed line) as a baseline for the determination of the anodic peak current. For the reverse sweep data the extended forward scan (dashed line with Cottrell decay) is folded backward (additionally accounting for capacitive current components) to serve as the baseline for the determination of the cathodic peak current.

This procedure can be difficult and an approximate expression for analysis based on the peak currents and the current at the switching potential has been proposed as an alternative. If the blank current before the anodic peak starts cannot be neglected, this current has to be extrapolated into the range where the peak occurs, or if possible, has to be subtracted from the sample voltammogram [44].

CV merits are, thus, largely in qualitative or diagnostic experiments. Quantitative measurements (of rates or concentration) are best obtained by employing step or pulse techniques.

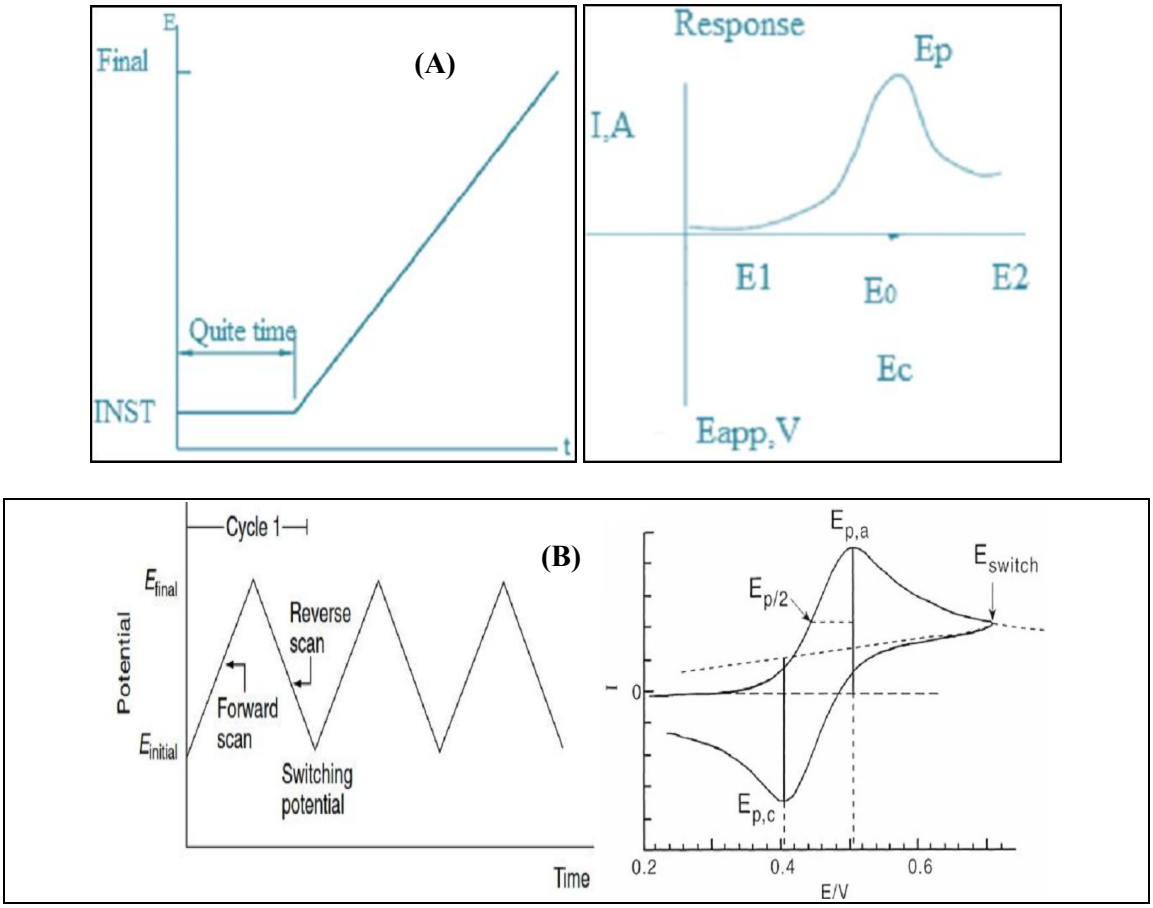

Figure 2.1: (A) Potential-excitation signal and voltammogram for LSV, (B) Potential–time excitation signal and Voltammogram with key parameters in a CV experiment**.**

For a reversible system, the anodic peak current, Ip,a, is given by the Randles–Sevcik equation (T = 25 ^{o}C) eq. (1) [44].

$$Ip,a = 2.69 \times 10^{5} n^{3/2} A D^{1/2} v^{1/2} C \ldots\ldots\ldots\ldots\ldots\ldots\ldots\ldots (1)$$

Where $I_{p,a}$ is the anodic peak current (in amperes),v is the scan rate (V s^{-1}), n is the number of electrons transferred per species, A is the electrode area (cm^2), D is the diffusion coefficient of the electroactive species (cm^2 s^{-1}) and C is the concentration of analyte in bulk solution (mol cm^{-3}). For a cathodic peak, Ip,c is given by the same expression but with a negative sign. Beyond the current peak, the current falls due to mass transport limitations to the electrode surface.

The value of E_p is useful in characterizing compounds and can be used for identification. The midpoint potential of the anodic and cathodic peaks in the CV is given by eq. (2) [44]:

$$E_{mid} = \frac{Ep,a + Ep,c}{2} = E^{0'} + \frac{RT}{nF} \ln \left(\frac{\sqrt{DRed}}{\sqrt{DOx}} \right) \ldots\ldots\ldots\ldots\ldots\ldots\ldots (2)$$

Where $E^{0'}$ is the formal potential, and DOx and DRed are the diffusion coefficients of the oxidized and reduced species. It can usually be assumed that DOx and DRed are equal and in such cases, the midpoint potential is nearly equal to the formal potential. The separation between anodic and cathodic peaks of the CV is given by eq. (3) [44, 47, 48]:

$$\Delta Ep - Ep,a - Ep,c - \frac{57}{n} mV \ldots\ldots\ldots\ldots\ldots\ldots\ldots (3)$$

Hence, in CV the peak separation can be used to determine the number of electrons per molecule of analyte oxidized or reduced, and as a criterion for Nernstian behaviour. In particular, if ΔEp is greater than 57/n mV then the reaction is not fully reversible [44].

Larger differences or nonsymmetric reduction and oxidation peaks are an indication of a quasi-reversible or irreversible reaction. For a quasi-reversible system, the electron transfer reaction does not respond instantaneously to a change in potential. The current is controlled by both charge transfer and mass transport.

Compared with a reversible voltammogram, the anodic peak is shifted to more positive potentials and the cathodic peak to more negative potentials. The quasi reversible CV parameters can be summarized as [47]: Ep is dependent on v, ΔEp depends on v and increases with v, Ip is linearly dependent on concentration and Ip depends on √v in a non-linear way, due to the transition from a reversible to an irreversible system.

Moving towards irreversible CV systems, when the kinetics has a successively greater effect in slowing the electron transfer, the current peaks become reduced in height and broader, and anodic and cathodic peak potentials become more widely separated. In the irreversible limit, no reverse reaction is observed, as happens with the oxidation of most pharmaceutical compounds. Totally irreversible electrochemical systems are characterized by a shift of the peak potential with the scan rate, according to eq. (4) [44]:

$$Ep = \frac{Ep,a + Ep,c}{2} = E^{0'} - \frac{RT}{\alpha nF} \left[0.78 - \ln \frac{K^0}{D^{1/2}} + \ln \left(\frac{\alpha nFv}{RT} \right)^{1/2} \right] \ldots\ldots\ldots\ldots\ldots\ldots\ldots (4)$$

Where α is the transfer coefficient, n is the number of electrons that are involved in the charge transfer step and k^0 is the standard rate constant of the electron transfer reaction.

For an irreversible process i.e. with sluggish electron transfer at the electrode surface, the peak current in CV is given by the Randles-Sevcik equation [49]. For an irreversible system, the peak current (I_p) is proportional to concentration and scan rate, eq. (5):

$$I_p = (2.99 \times 10^5) n(\alpha n_a)^{1/2} AC^* D^{1/2} v^{1/2} \text{.....(5)}$$

Where n - is the overall electron transfer, na- the number of electrons in the rate determining step of the electrode process, α - is the transfer coefficient, A - the electrode area, C*- bulk concentration, D - diffusion coefficients of the electroactive species, and *v* - scan rate. The peak current is directly proportional to the concentration of the analyte and the scan rate. For a well-behaved system, the anodic and the cathodic peak currents are equal, and the ratio (I_{pa}/I_{pc}) is 1.0. The half-wave potential, $E_{1/2}$, is midway between the anodic and cathodic peak potentials. In this irreversible case, LSV and CV are equivalent. The parameters for irreversible reactions can be given as [47].

(A) Ep depends on v, (B) Ip is proportional to √v, (C) Ip is linearly proportional to concentration.

For irreversible systems, the peak potentials of anodic or cathodic processes are shifted toward more positive or negative potential values, respectively. In many cases, the value of na = 1.

Typical scan rates are between 25 and 1,000 mV s^{-1} for analytical purposes. The detection limits of CV and LSV are usually about 10^{-6} M so that these techniques are not sensitive enough to determine drugs in body fluids after therapeutic doses [44].

2.2.1.3 Differential Pulse Voltammetry

Differential Pulse Voltammetry (DPV) is a very useful technique for measuring trace levels of organic and inorganic species [41]. A potential waveform for DPV is fixed magnitude pulses, superimposed on a slowly changing base potential, applied to the working electrode.

The DPV technique was proposed by Barker and Gardner [50] for the DME in order to enable lower detection and quantification limits for electrochemically active compounds. DPV is one of the most sensitive voltammetric techniques because the charging current is strongly discriminated against for the faradaic current, and the ratio of faradaic to charging current is large. At solid electrodes, a better response is seen in many cases, especially involving organic pharmaceutically active compounds, allowing the detection of analytes

present in solution at a concentration as low as 10^{-8} M. The higher sensitivity of DPV than of NPV is from differential current sampling with constant height, small pulses.

In DPV potential, pulses of fixed, small amplitude (between 10 and 100 mV) are superimposed on a changing base potential (Fig. 2.2A). DPV is measured current at two points; before the application of the pulse, and at the end of the pulse. The first current is subtracted from the second, and the current difference $\{\Delta i = i(t_2) - i(t_1)\}$ is plotted versus the applied potential [41, 51]. In typical conditions, the potential is changed from an initial value in small steps (between 2 and 5 mV), and a voltage pulse (pulse width) of short duration (50 ms) is superimposed at the end of a long step (between 0.5 and 5s) [52].

A consequence of double sampling and representing ΔI against potential is that the DPV curves are peak-shaped, and the peak height is directly proportional to the concentration of electroactive species. In a differential pulse voltammogram, Figure 3 A, the peak potential, Ep, can be related to $E_{1/2}$, and Ep can be used for the identification and an indication of the reversibility or irreversibility of the system. With increasing irreversibility, Ep moves away from the reversible value of $E_{1/2}$, at the same time as the peak width increases and peak height diminishes. The peak potential (Ep) for oxidation is related to $E_{1/2}$ by the following equation (6):

$$E_p = E_{1/2} - \frac{\Delta E}{2} \quad \ldots\ldots\ldots\ldots\ldots\ldots\ldots\ldots\ldots\ldots (6)$$

Where, ΔE is the pulse amplitude, the negative sign being replaced by a positive sign for a reduction. Thus, for an oxidation process the peak is shifted in the negative direction as the pulse amplitude increases and for a reduction in the positive direction. As ΔE increases, some deviations from theoretical calculations occur. The faradaic current increases linearly with ΔE in the small-amplitude region, as does the double layer charging current. Increasing the amplitude of ΔE improves signal response and the signal-to-noise ratio whilst the faradaic to charging current ratio stays constant. The highest of the produced peak current is proportional to the concentration of analyte eq. (7) [41, 51].

$$I_d = \frac{nFAD^{\frac{1}{2}}C}{\sqrt{(\pi t_m)}}\left(\frac{1-\sigma}{1+\sigma}\right) \quad \ldots\ldots\ldots\ldots\ldots\ldots\ldots\ldots\ldots\ldots (7)$$

Where σ = exp ((nF/RT) (ΔE/2)) and ΔE is pulse amplitude.

As ΔE increases, the quotient (1- σ/1+σ) increases and finally reaches unity, but resolution may become worse. The selection of pulse amplitude and potential scan rate usually requires a tradeoff between sensitivity, resolution, and speed and should be done in agreement with the theory [52]. Larger pulse amplitudes can lead to broader peaks, the pulse width (t_m) is usually set at about 50 ms and pulse amplitudes of 25–50 mV coupled with a 5 mV s^{-1} scan rate are commonly employed in electroanalytical studies. The DPV peak shape and current magnitude are strongly influenced by the chemical and electrochemical steps involved in the electrode process. This can have important implications in electroanalytical applications to pharmaceutically active compounds. According to Wang et al. (2018), Nitrogen-doped carbon nanotubes decorated poly (L-Cysteine) as a novel, ultrasensitive electrochemical sensor for simultaneous determination of theophylline and caffeine, TP and CAF with a linear range from 0.10 to 70.0 μM and 0.40–140.0 μM, low detection limit (S/N = 3) of 0.033 μM, and 0.20 μM, respectively [53].

2.2.1.4 Square Wave Voltammetry

Square wave voltammetry (SWV) is one of the major voltammetric techniques in current use for electroanalysis. SWV is a powerful electrochemical technique that can be applied in both analytical and kinetic electrochemical measurements [44]. SWV is a large amplitude differential technique in which a waveform is composed of a symmetrical square wave, superimposed on a staircase and is applied to the working electrode [54]. The current is sampled twice during each square-wave cycle, once at the end of the forward pulse (If), once at the end of the backward pulse (Ib), and the total net (It = If - Ib) currents (Fig. 2.2B). The difference between the two measurements is plotted vs. the staircase potential. The resulting peak-shaped voltammogram displays excellent sensitivity and effective discrimination against background contributions [47, 55, 56].

The advantage of SWV is that a response can be found at a high effective scan rate, thus reducing the scan time. Because of this advantage, SWV is employed more often than other pulse techniques. There are advantages: greater speed in analysis and lower consumption of electroactive species with DPV, and reduced problems with blocking of the electrode surface. SWV is similar to DPV in that current (I) samples at two different times in the waveform and results in a differential output. The forward current is measured just before the down pulse is applied. The reverse current is measured at the end of the reverse pulse. The currents are

measured during the last few microseconds of each pulse and the difference between the current is measured on two successive as a net response. The net current is defined from differences between forward and reverse current. The sensitivity increases from the fact that the net current is larger than either the forward or reverse components. Also, the sensitivity of SWV is mostly higher than that of DPV [55].

SWV provides several advantages to the electro analyst. First, the application of the SWV waveform is that the detrimental effects of charging current are reduced and so the scan rate can be increased drastically. The second advantage of SWV is oxygen need not be excluded from the analyte solution; provided the voltammetric peak is more cathodic than that for the reduction of oxygen, then the magnitude of both forward and reverse current will incorporate an equal current due to the reduction of oxygen. The other advantage of SWV, the difference of currents is larger than either forward or reverse current, so the height of the peak is usually quite easy to read, thus increasing the accuracy [44].

The major advantage of SWV is its speed. SWV has very low detection limits of about 10^{-8} M for fast electrode kinetics, and the theoretical sensitivity is 4 and 3.3 times higher than the DPV response, for reversible and irreversible systems, respectively [44, 57].

The application of SWV has become very popular in the last decade, it is highly sensitive to surface-confined electrode reactions and the theory is well-developed. According to Mekassa et al. (2017), simultaneous determination of CAF and TP using SWV at modified P(LeAsp)/f-MWCNTs/GCE electrode, with a limit of detection of CAF and TP 0.28 and 0.02 μM (S/N = 3), in the range of 1–150 and 0.1–50 μM respectively [28].

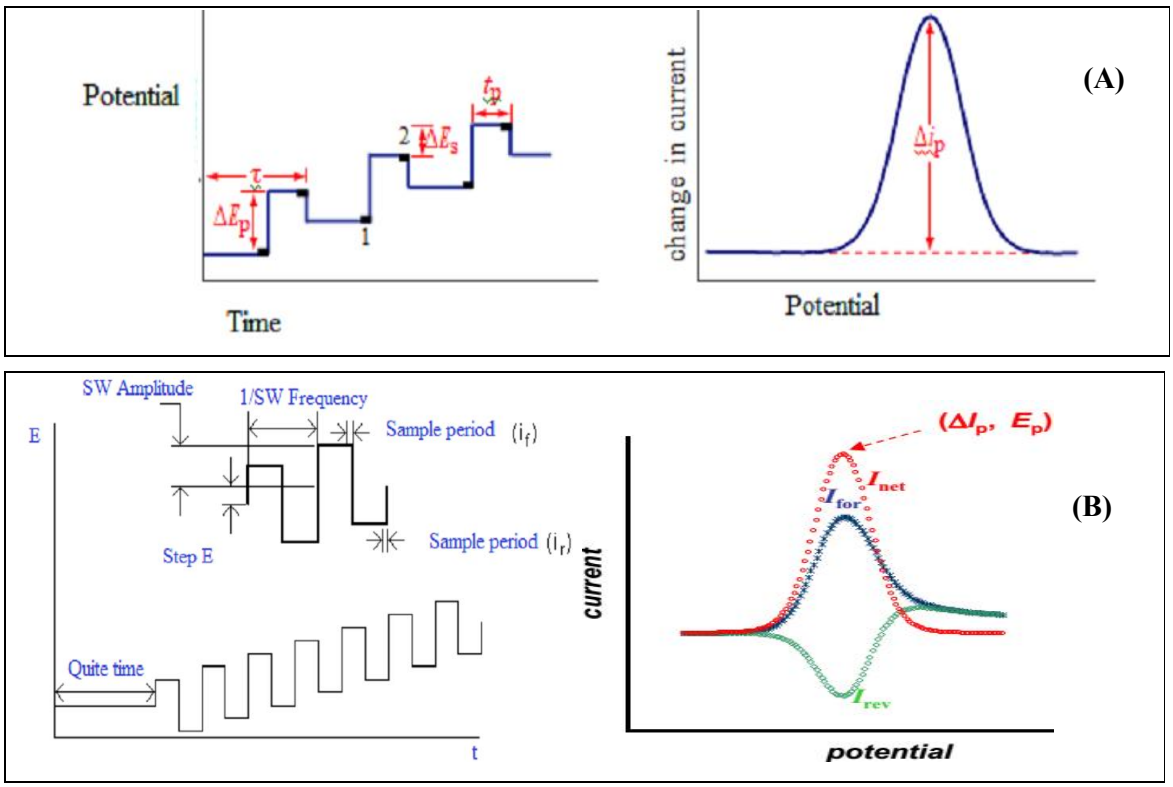

Figure 2.2: (A) Potential-excitation Signals and voltammograms for DPV, (B) SWV: potential–time waveform and SWV of a reversible reaction (A. forward, B. reverse and C. net current)

2.2.1.5 Stripping Voltammetry

Pre-concentration of an analyte on the electrode surface enables the detection limits to be lowered further down to 10^{-10}–10^{-12} M by using pulse voltammetric methods in the determination step, following the pre-concentration [58]. Such methods are normally known as stripping voltammetry (SV). SV is composed of the three most common techniques, namely anodic, cathodic, and adsorptive voltammetric stripping [42, 58].

SV has two steps in common; the first step, the analyte species in the sample solution is concentrated onto or into a working electrode. It is this crucial preconcentration step that results in exceptional sensitivity that can be achieved. During the second step, the preconcentrated analyte is measured or stripped from the electrode by the application of a potential scan. Any number of potential waveforms can be used for the stripping step (the most common are DPV and SWV) due to the discrimination against charging current [42]. SV is the most sensitive technique for the study of trace analysis of many metals and

compounds in environmental samples, clinical and industrial [42, 59]. Important conditions that should be held constant include the electrode surface, rate of stirring, and deposition time [42].

2.2.2 Types of Working Electrodes

2.2.2.1 Mercury Electrodes

For stripping analysis, the working electrode must be stationary and have a favorable redox behavior of the analyte, reproducible area and low background current over a wide range of potential. The most used electrode, which fulfills these requirements, is hanging dropping mercury electrode and mercury film electrode [46].

2.2.2.2 Solid Electrodes

The limited anodic potential of mercury electrodes has precluded their utility for monitoring oxidizable compounds. Accordingly, solid electrodes with extended anodic potential windows have attracted considerable analytical interest. There are many different types of solid electrodes used as working electrodes such as gold, platinum, glassy carbon electrode, carbon paste electrode, carbon fiber electrode, and epoxy-bonded graphite electrode. Unlike mercury electrodes, solid electrodes present a heterogeneous surface with respect to the electrode chemical activity. Such surface heterogeneity leads to deviations from the behavior expected from homogenous surfaces [46].

An important factor in using solid electrodes is the dependence of the response on the surface state of the electrode. Accordingly, the use of such electrodes requires precise electrode pretreatment and polishing to obtain reproducible results.

2.2.2.3 Chemically Modified Electrodes

The used working electrode may be insensitive to be applied in a certain field. Modification will be used to improve the properties of the selected working electrode. The main idea of the modification depends on incorporating a reagent on the electrode surface or into the matrix of the selected electrode [60].

The most famous method for the incorporation of a modifier to the electrode surface is covering the electrode surface with suitable polymer film. This may occur by covering the electrode surface with the solution of the selected polymer and allowing the solvent to

evaporate. Also, electropolymerization may be used to make the polymer film on the electrode surface.

As a new type of CMEs, pre-concentrated CMEs were described [60]. Such modified electrodes have surfaces characterized by the ability for reacting and binding the target analyte. Preconcentrating agent used in such modifications is usually incorporated in the electrode matrix (as done with carbon paste electrode [61] or may be binding with functionalized polymeric film on the electrode surface.

Types of modified electrodes can be prepared in the following ways;

A) Chemical modification: The electrode surface is activated by chemical reaction, such as silane, which is then used to react with another chemical species that becomes immobilized on the surface [62, 63].
B) Adsorption: This is used for coating electrode surfaces with solutions of the modifier either by dipping or, more commonly, by applying a drop of the solution followed by spinning to evaporate the solvent (spin coating). This is particularly used for modifying soluble polymers. Some polymeric species which have a tendency for self-assembly can also be applied through such procedures, leading to self-assembled monolayers on the electrode surface [63].
C) Electro adsorption and electrodeposition: The deposition of the substance on an electrode by the action of electricity (especially by electrolysis). If adsorption is carried out under the influence of an applied potential then thicker modifier layers usually result, but there is probably a greater guarantee of uniformity. Such procedures are used for the formation of conducting polymers [63].
D) Plasma: The electrode surface is cleaned by plasma leaving the surface with dangling bonds and being highly active. Adsorption of any species, such as amines or ethenes, in the vicinity, is very fast [63].
E) Electropolymerization: Used for the modification of electrode surfaces that can accelerate the transmission of electrons onto the surface of the electrode, it has high sensitivity and selectivity, because of the film homogeneity in electrochemical deposition, and it has a strong adherence to the electron surface and large surface area [64].

3 MATERIALS AND METHODS

3.1 Chemicals and Apparatus

Nitric acid (65%, UNI- CHEM), alumina powder, sodium acetate anhydrous (99%,) caffeine anhydrous (99%) and hydrochloric acid (36%, Loba Chemie), sulfuric acid (98%, Fisher scientific, UK), acetic acid (99%, Fisher chemical, UK), theophylline anhydrous (99%), paracetamol (99%) and ephedrine (99%, Sigma Aldrich), sodium hydroxide (97%, Blulux Laboratories Ltd), ascorbic acid (99%), sodium chloride (99%), and potassium chloride salts (99.5%, Blulux laboratories(p) Ltd), glucose (99%, Blulux ® the best ALab can Get), urea (99%, Titan Biotech Ltd. India), $K_3[Fe(CN)_6]$ and $K_4[Fe(CN)_6]$ (98.0%, BDH laboratories supplies, England), poly(aquachlorobis(1,10-phenanthroline)cupper(II)iodidemonohydrate) or poly(ACP_2CuIH) complex, were used. All chemicals were of analytical grade that they were used without further purification. Distilled water was used throughout the work.

While electrochemical experiments were conducted using CHI760E electrochemical workstation (Austin, Texas, USA) with a conventional three-electrode system at room temperature. Poly(ACP_2CuIH)/GCE or bare glassy carbon electrode, platinum coil, and Ag/AgCl (3.0 M KCl) were employed as working, auxiliary, and reference electrodes, respectively. The hot plate, deionizer (Evoqua water technologies), pH meter (Adwa model AD8000), electronic balance (Nimbus, ADAM equipment, USA), centrifuge (centurion scientific. Ltd. West Sussex, UK, model 1020D) and refrigerator (Lec refrigeration PLC, England) were used to extract a sample, sample preparation, adjust the pH of a solution, measure mass, during blood serum preparation, and preserve samples, respectively and among the materials were used in this work.

3.2 Procedure

3.2.1 Electrode Modification

Poly(ACP_2CuIH)/GCE was synthesized following the procedure reported [29]. Briefly: Glassy carbon electrode was mirror polished with 1.0, 0.3 and 0.05 μm alumina powder, successively and then washed thoroughly with distilled water. Poly(ACP_2CuIH) was deposited on the surface of the polished GCE potentiodynamically by scanning the potential between -1.2 to +1.8 V at a scan rate of 100 mV s^{-1} for 15 cycles in pH 7.0 PBS containing 1.0 mM ACP_2CuIH. Then, the modified electrode was rinsed with distilled water and

conditioned by sweeping it in 0.5 M H_2SO_4 between -0.8 to +0.8 V at 100 mV s^{-1} until a stable voltammogram is obtained.

3.2.2 Electrochemical Measurements

A conventional three electrode cell, consisting of bare GCE or poly(ACP_2CuIH)/GCE as working, Ag/AgCl, KCl (3.0 M KCl) as a reference, and a platinum coil as the auxiliary electrode, were used for electrochemical measurements. All potentials mentioned in this paper refer to the Ag/AgCl (3.0 M KCl) reference electrode.

3.2.3 Preparation of Standard Stock and Working Solutions

Stock solutions of CAF and TP, each with 10.0 mM concentration, were prepared in a 100 mL volumetric flask by dissolving 194.2 mg of CAF and 180 mg of TP in distilled water. An equi-molar (1.0 mM) mixture of CAF and TP pH 5.0 of 0.1 M ABS was prepared by mixing measured volumes of each from the respective stock solution. Finally, the individual and mixed equi-molar standard TP and CAF working solutions of the various concentration (1.0, 5.0, 10.0, 20.0, 40.0, 80.0, 120.0, 160.0, and 200.0 μM) were prepared from the stock solution by serial dilution using the optimized pH 4.5 of 0.1 M ABS [18, 28].

3.2.4 Preparation of Real Samples

3.2.4.1 Tablet Sample

Panadol extra (gsk Dungarvan, Ireland) tablets labeled 65 mg CAF/tablet, and Theodrine tablets (Addis pharmaceutical factory, Ethiopia) labeled 120 mg TP/tablet were purchased from a local drug store in Bahir Dar, Ethiopia. Five randomly selected tablets from each tablet brand (with an average tablet mass of 695 mg Panadol extra and 298 mg Theodrine) were ground and homogenized with mortar and pestle. A stock solution of 2.0 mM CAF in tablet sample was prepared by dissolving accurately weighed 415 mg Panadol extra tablet powder in 25 mL double distilled water, filtered, and then transferred to 100 mL volumetric flask and filled up to the mark with double distilled water. 2.0 mM TP in tablet stock solution was also prepared following the same procedure as for CAF except the mass of Theodrine taken was 89 mg. Further, working tablet solution samples with a nominal concentration of 80 μM of TP and CAF in pH 4.5 ABS were prepared from the respective tablet stock solutions [18, 28]. All tablet samples spiked with equi-molar (80 μM) mixture of TP and CAF were prepared in the same way and compared the results.

3.2.4.2 Tea Sample

Accurately weighed 5 g of each analyzed tea sample (Black Lion (East Africa Agribusiness plc), Addis, and Wush Wush tea samples (Ethio Agri-CEFT PLC), all purchased from a local supermarket in Bahir Dar, Ethiopia) was transferred into 100 mL of water, boiled at 80 °C for 30 min to extract TP and CAF. After filtration, 2.5 mL of the filtrate was put in a 50 mL volumetric flask and diluted to the mark with pH 4.5 ABS. All tea samples spiked with equi-molar (100 μM) mixture of TP and CAF were prepared in the same way as real tea samples.

3.2.4.3 Human Blood Serum Sample

A human blood sample was obtained from a healthy volunteer at the Felege Hiwot Referral Hospital, Bahir Dar, Ethiopia. About 5.0 mL fresh sample of blood was taken and centrifuge at 1500 rpm for 20 min to remove all precipitating materials. Three serum samples were then prepared for real sample analysis of TP and CAF and recovery tests. A serum sample for detection of TP and CAF was prepared by transferring 0.25 mL of the serum to 25 mL and filled to the mark with pH 4.5 ABS. Two other serum samples for the recovery test were prepared in the same way as the blank except that the first was spiked with a volume of a mixture of TP and CAF with a resulting concentration of 80 μM each while the second 120 μM TP and CAF.

4 RESULTS AND DISCUSSION

4.1 Fabrication and Characterization of Poly(ACP_2CuIH)/GCE

Poly(ACP_2CuIH)/GCE film modified glassy carbon electrode was fabricated following the procedure reported [29]. During the potentiodynamic electrodeposition of the polymer film on the electrode surface (Fig. 4.1), cathodic peak (peak-a') at -0.24 V and anodic peaks (peak-a, b, c, and d) at 0.08, 0.5, 0.8, and 1.2 V, respectively were observed whose current increased with increasing scan cycles indicating polymer film growth. Inset of Fig. 4.1(A) curves a & b) depicts the voltammograms of (a) first cycle and (b) fifteenth cycle showing the current increment with scan numbers and hence deposition of polymer film. Inset of Fig. 4.1(B) depicts the CVs of bare GCE (curve 2) and stabilized poly(ACP_2CuIH)/GCE (curve 1) in a monomer free 0.5 M of H_2SO_4 solution between -0.8 to +0.8 V. Appearance of three visible peaks at poly(ACP_2CuIH)/GCE whereas no visible peaks except a reductive peak for molecular oxygen reduction at the unmodified GCE is clear confirmation for deposition of an electroactive polymer film at the surface of the electrode (Inset of Fig. 4.1(B)).

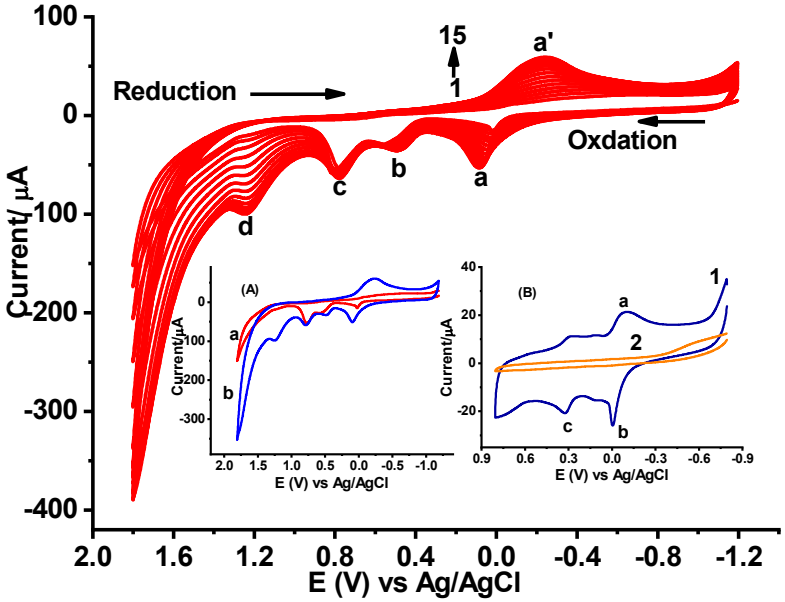

Figure 4.1: Cyclic voltammograms of GCE in pH 7.0 PBS containing 1.0 mM poly(ACP_2CuIH)/GCE scanned between -1.2 and +1.8 V for 15 cycles at a scan rate of 100 mV s^{-1}. Inset: (A) CVs of (a) first cycle and (b) fifteenth cycle, (B) CVs of (2) bare GCE, and (1) stabilized poly(ACP_2CuIH)/GCE in monomer free 0.5 M H_2SO_4 scanned between -0.8 and 0.8 V at scan rate of 100 mV s^{-1}.

4.2 Characterization of Poly(ACP_2CuIH)/GCE

The modified electrode was characterized by two techniques; cyclic voltammetry (CV) and electrochemical impedance spectroscopy (EIS).

4.2.1 Characterization by Cyclic Voltammetry

Cyclic voltammetry using $[Fe(CN)_6]^{3-/4-}$ as a probe was used to characterize the poly(ACP_2CuIH)/GCE modified glassy carbon electrode (Fig. 4.2). In contrast to the redox peaks with peak potential difference (ΔE) of 424 mV at the unmodified electrode, appearance of couple of redox peaks with much enhanced current and reduced potential difference (ΔE) of 96 mV at the poly(ACP_2CuIH)/GCE for $[Fe(CN)_6]^{3-/4-}$ indicated catalytic property of the polymer film towards $[Fe(CN)_6]^{3-/4-}$ redox reaction. The observed catalytic effect of the polymer modified electrode might be ascribed to the reported increased electrode effective surface area of the modified electrode [29].

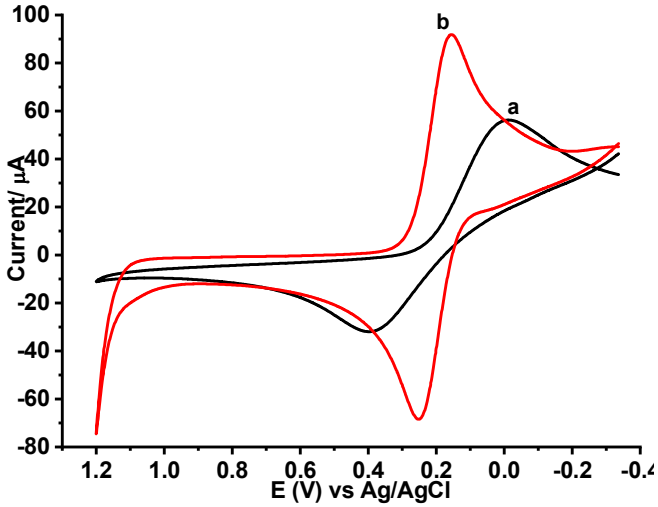

Figure 4.2: CVs of unmodified (a) and modified (b) GCEs in pH 7.0 PBS containing 10 mM $[Fe(CN)_6]^{3-/4-}$ and 0.1 M KCl at scan rate of 100 mV s^{-1}.

4.2.2 Characterization by EIS

Figure 4.3 presents the Nyquist plot of both unmodified and modified electrodes in $[Fe(CN)_6]^{3-/4-}$. As can be seen from the (Fig. 4.3), both electrodes showed a Nyquist curve with a semi-circle of different diameter and hence different charge transfer resistance in the high frequency region and a linear line in the low frequency region showing the diffusion of the

electroactive species from the bulk of solution towards the electrode surface. The reduced peak-peak separation (ΔE 96 mV) for the probe at the modified electrode (curve b of Fig. 4.2) than at the unmodified electrode (ΔE 424 mV) could be ascribed to the lower charge transfer resistance of the modified (curve b of Fig. 4.3) than of the unmodified electrode (curve a of Fig. 4.3)

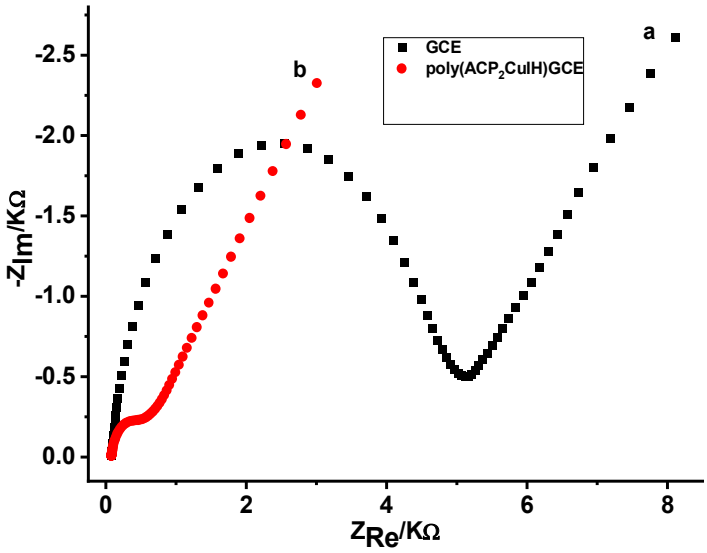

Figure 4.3: Nyquist plots for (a) bare GCE and (b) poly(ACP_2CuIH)/GCE in pH 7.0 PBS containing 10.0 mM $[Fe(CN)_6]^{3-/4-}$ and 0.1 M KCl at frequency range: 0.01–100,000 Hz, applied potential: +0.23 V, and amplitude: 0.01 V.

The presumed RC-parameters (R_s, R_{ct}, and C_{dl}) for the studied electrodes as calculated using eq. (8) from the respective semi-circles is summarized in Table 4.1.

$$C_{dl} = \frac{1}{2\pi R_{ct} f_{max}} \quad \ldots\ldots\ldots\ldots\ldots\ldots (8)$$

where f_{max}, is the frequency (Hz) corresponding to the maximum value of –Z" at the semi-circle (316.2 Hz for GCE and 40.7 Hz for modified GCE), C_{dl} is the double layer capacitance, R_{ct} is the charge transfer resistance given by the diameter of the semi-circle, and R_s is solution resistance given by the x-axis value corresponding to the semicircle at maximum frequency.

While higher double layer capacitance (C_{dl} = 4.70 × 10^{-6} F) of the modified electrode indicates deposition of a certain material on the surface of the electrode, lower charge transfer resistance value (R_{ct} = 830.7 Ω) indicated surface modification by a more conductive material

which is responsible to lower the redox potentials of an electroactive species. The roughness factor (RF) of poly(ACP_2CuIH)/GCE is then calculated from the double-layer capacitance according to the eq. (9) below.

$$RF = \frac{C_{dl}}{C_S} \tag{9}$$

C_S in eq. (9) is the electrochemical double-layer capacitance of a smooth and planar electrode surface of the same material measured under the same conditions and C_{dl} is double layer capacitance of modified electrode. Then 52.4 times surface roughness of modified electrode greater than unmodified electrode. Therefore, the results obtained from the EIS data are in support of the effects of the modified electrode towards $[Fe(CN)_6]^{3-/4-}$ probe confirming the modification of the surface of the electrode by an intrinsically conducting polymer film.

Table 4.1 Summary of the calculated values of the RC- parameters:

Electrode type	R_s (Ω)	R_{ct} (Ω)	Frequency (Hz)	C_{dl} (F)	RF
Bare GCE	50.7	5615	316.2	8.97×10^{-8}	52.4
Poly(ACP_2CuIH)/GCE	50.7	830.7	40.7	4.70×10^{-6}	

4.3 Cyclic Voltammetric Study of TP and CAF at Poly(ACP_2CuIH)/GCE

4.3.1 Electrochemical Behavior of TP and CAF at Poly(ACP_2CuIH)/GCE

The electrochemical behavior of a mixture of 1.0 mM TP and 1.0 mM CAF in 0.1 M acetate buffer (pH 5.0) was investigated (Fig. 4.4). Both TP and CAF showed irreversible oxidation at both the unmodified and polymer modified glassy carbon electrodes although with different current intensity and peak potential. In contrast to the weakly separated oxidative peaks for TP and CAF at the unmodified electrode (curve A of inset), appearance of well separated peaks with enhanced current at relatively lower potential for each at the modified electrode (curve B of inset) was ascribed to the catalytic property of the modifier towards oxidation of TP and CAF. Moreover, appearance of well resolved oxidative peaks sufficiently separated (220 mV) at the polymer modified electrode indicated potential applicability of the method for simultaneous detection of TP and CAF.

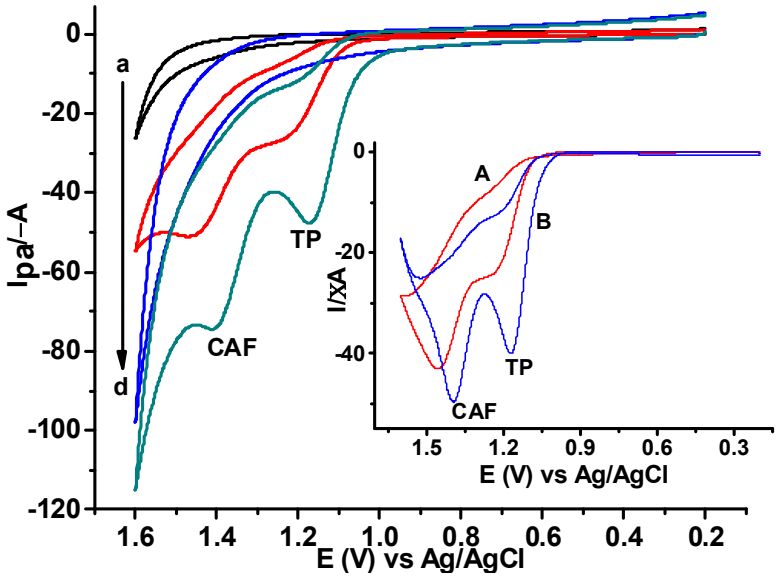

Figure 4.4: CVs of bare GCE (a, c) and poly(ACP_2CuIH)/GCE (b, d) in 0.1 M ABS pH 5.0 containing no (a, b) and 1.0 mM CAF and TP (c, d) at scan rate of 100 V s^{-1}. Inset: corrected for blank CVs of (A) bare GCE, and (B) poly(ACP_2CuIH)/GCE.

Generally, the peak current of TP (24.0 µA) and CAF (42.9 µA) at the unmodified electrode increased to 39.8 for TP and 49.6 µA for CAF at the modified Poly(ACP_2CuIH)/GCE indicating the electrocatalytic activity of the modifier towards oxidation of TP and CAF. The improved electrocatalytic performance of poly(ACP_2CuIH)/GCE might be attributed to the electrostatic interaction between the surface modifier and the analytes or the increased effective surface area of the modified surface as reported elsewhere [29].

4.3.2 Effect of Scan Rate on the Peak Current and Peak Potential of CAF and TP

The effect of scan rate on the simultaneous oxidation of TP and CAF at the poly (ACP_2CuIH)/GCE was investigated (Fig. 4.5). The observed peak potential shift in the positive direction with scan rate for both TP and CAF confirmed irreversibility of the oxidation reaction they undergo (Fig. 4.5A). Better determination coefficient value (R^2) for dependence of oxidative peak current of both TP and CAF on square root of scan rate (0.99890 & 0.99953, respectively) (Fig. 4.5C) than on scan rate (0.99553 & 0.96040, respectively) (Fig. 4.5B) suggested that the oxidation of TP and CAF at the electrode surface is predominantly a diffusion-controlled process [27, 65]. Furthermore, slope values of 0.42 and 0.47 for plot of log (peak current) versus log (scan rate) (Fig. 4.5D), which is very close

to the ideal 0.5 value for diffusion control, confirmed the diffusion mass transport kinetics of the oxidation of both TP and CAF at the polymer modified electrode [26].

In addition, the influence of scan rate on the oxidation peak potential (Epa) was investigated. With increasing scan rate, Epa of the two species shifted to more positive potentials (Fig. 4.5A). Dependence of Epa on natural logarithm of scan rate analysis of (Fig. 4.6) showed slope of 0.03 for TP and 0.035 for CAF for the respective plot of peak potential (Ep_a) versus the natural logarithm of scan rate (lnv), (Epa (V) = 1.1+ 0.03 lnv (mV s^{-1} with R^2 = 0.99282 for TP, and Epa (V) = 1.3 + 0.035 lnv (mV s^{-1}) with R^2 = 0.99903 for CAF). This indicated that the oxidation of TP and CAF at poly(ACP_2CuIH)/GCE surface is an irreversible reaction [27, 47, 66, 67].

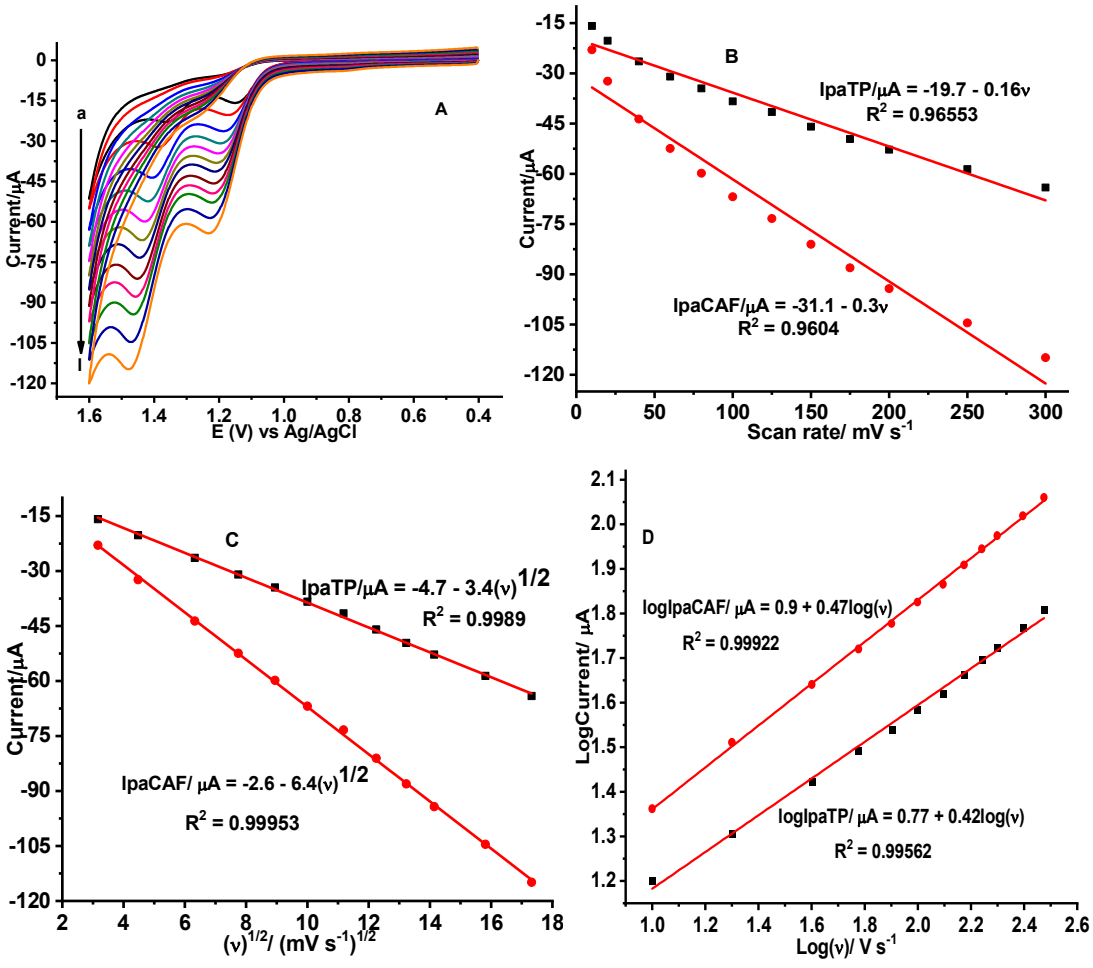

Figure 4.5: (A) CVs of poly(ACP_2CuIH)/GCE in pH 5.0 ABS containing equi-molar (1.0 mM) mixture of TP and CAF at various scan rates (a–l: 10, 20, 40, 60, 80, 100, 125, 150, 175, 200, 250 and 300 mV s^{-1}, respectively), plot of (B) Ip vs. ν, (C) Ip vs. $\nu^{1/2}$, and (D) log (Ip) vs. log (ν).

The relationships between Ep_a and lnν were as follows: the slope of 0.03 for TP and 0.035 for CAF, (Fig. 4.6). Since only oxidation peak appeared in the CV of TP and CAF, the redox reactions on the surface of poly(ACP_2CuIH)/GCE were irreversible, according to the Nicholson equation (4):

$$Ep = \frac{Ep,a + Ep,c}{2} = E^{o'} - \frac{RT}{\alpha nF}\left[0.78 - \ln\frac{K^0}{D^{1/2}} + \ln\left(\frac{\alpha nF\nu}{RT}\right)^{1/2}\right] \ldots\ldots\ldots\ldots\ldots\ldots\ldots (4)$$

Where α is the electron transfer coefficient, n is the number of electron transfer, T is the absolute temperature (298 ^oC), F is Faradic constant, R is gas constant (8.314 J. mol^{-1} k^{-1}), D is the diffusion coefficient, K is the apparent electron transfer rate constant, and n is the number of electrons which are involved in the charge transfer step. The linear slope of the Epa vs. lnν curve was equal to ($slope = RT/\alpha nF = 0.03$) for TP. For irreversible processes, α is generally assumed to be about 0.5 [39]. Therefore, n, is the oxidation reaction of TP could be inferred to be $1.7 \approx 2$.

The oxidation reaction of CAF electron number is the linear slope of the Epa vs. lnν curve was equal to ($slope = RT/\alpha nF = 0.035$). So, $n = 1.5 \approx 2$.

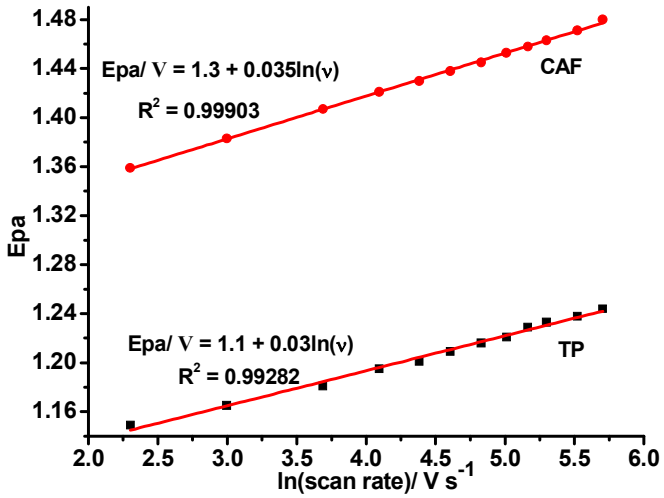

Figure 4.6: Plot of Ep_a vs. lnv/ V s^{-1} of poly(ACP_2CuIH)/GCE in pH 5.0 ABS containing equi-molar (1.0 mM) mixture of TP and CAF at various scan rates (a–l: 10, 20, 40, 60, 80, 100, 125, 150, 175, 200, 250 and 300 mV s^{-1}, respectively).

4.3.3 Effect of pH on Peak Current and Peak Potential of TP and CAF

A redox reaction of organic compounds mainly depends on the pH of the buffer solution [6]. Hence, the effect of 0.1 M pH 5.0 of supporting electrolyte, acetate buffer solution (ABS) [33] on the peak current and peak potential of TP and CAF was investigated.

The effect of pH of 0.1 M acetate buffer solution (ABS) on the peak current and potential of TP and CAF at the polymer modified electrode was further investigated in the range from 3.0 to 6.0 (Fig. 4.7A). The peak current of both TP and CAF decreased slowly with increasing the pH of the supporting electrolyte (Fig. 4.7C). Taking the peak current increment, low background current, accompanied peak shape distortion, and peak potential separation into consideration, pH 4.5 was selected as the optimum pH for further analyses. This trend could be attributed to electrostatic attraction between the poly(ACP_2CuIH)/GCE electrode modifier (pKa of phenanthroline 4.86) [29] and the positively charged CAF (pka = 10.4) [33] & TP (pka = 8.8) [18].

The dependence of the peak potential (Ep) of TP and CAF on the pH of buffer solution was also examined. The peak potential of TP and CAF shifted almost linearly towards negative potentials with increasing the pH (Fig. 4.7A) indicating participation of protons during their oxidation at the modified electrode. As presented in Fig. 4.7B, plot of peak potentials vs. pH values in the range of 3.0 to 6.0 revealed regression equations of Epa (V) = −0.04826pH + 1.4066, and Epa (V) = −0.017pH + 1.49 for TP, and CAF, respectively (Fig. 4.7B). While the slope of −0.048 for TP, which is close to the theoretical Nernstian value of 0.059 V, suggested an oxidation process that involves equal number of electrons and protons in a 1:1 ratio [17, 39]; slope of −0.017 for CAF is too lower than the ideal value of 0.059 V for a 1:1 ratio of proton and electron involvement. This might be an indication for the oxidation of CAF without the involvement of protons as is reported by previous works [17, 39, 47].

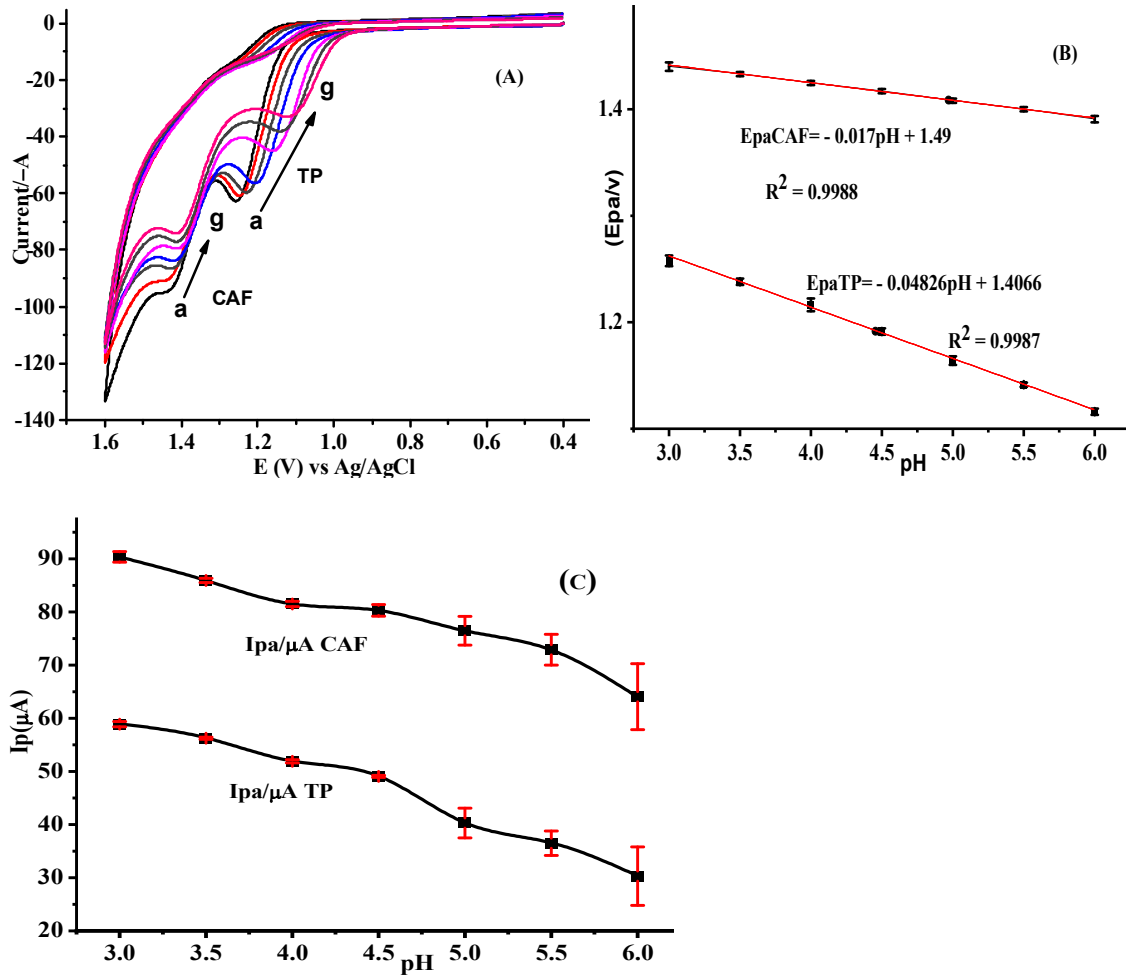

Figure 4.7: (A) Representative CVs of poly(ACP_2CuIH)/GCE in ABS of various pHs (a–g: 3.0, 3.5, 4.0, 4.5, 5.0, 5.5, and 6.0, respectively) containing equi-molar (1.0 mM) mixture of TP and CAF, plot of mean ($\bar{x} \pm$ %RSD) (B) Ep and (C) Ip vs. pH in the entire pH range.

4.4 SWV Investigation of TP and CAF at Poly(ACP_2CuIH)/GCE

Square wave voltammetry (SWV) is known to be more powerful to discriminate the Faradaic current from the non-Faradaic current than cyclic voltammetry [68]. SWV was used for simultaneous quantification of CAF and TP in human serum, tea and tablet samples. Figure 4.8 presents square wave voltammograms of equi-molar mixture of TP and CAF in pH 4.5 ABS at both the unmodified GCE and ploy(ACP_2CuIH)/GCE. In contrast to the peak at the unmodified electrode (Fig. 4.8 curve a), appearance of peaks with ≈160% CAF and ≈350% TP current enhancement at reduced potentials (ΔE 70 mV for TP and ΔE 190 mV for CAF) at

poly(ACP_2CuIH)/GCE confirmed the catalytic contribution of the polymer film towards the oxidation of CAF and TP (Fig. 4.8 curve b).

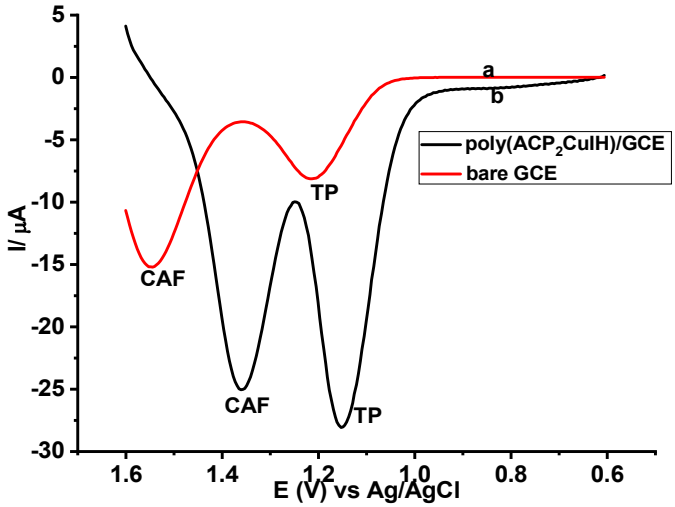

Figure 4.8: Corrected for blank SWVs of (a) bare GCE and (b) poly(ACP_2CuIH)/GCE in pH 4.5 ABS containing 1.0 mM TP and CAF at step potential: 6 mV, amplitude: 35 mV, and frequency: 20 Hz.

4.4.1 Optimization of Square Wave Voltammetric Parameters

The dependence of peak current response of the polymer modified electrode for TP and CAF in ABS of pH 4.5 on square wave parameters such as step potential, amplitude, and frequency were investigated and optimized. The step potential was measured in the range of 2–10 mV by fixing the frequency at 15 Hz and amplitude at 25 mV (Fig. 4.9A). The peak height increases as the step potential increases, exhibiting a maximum at 6 mV, after which it decreases accompanied by broadening of peak width. Therefore 6 mV was chosen as the optimum SWV step potential (inset Fig. 4.9A). The amplitude was also optimized in the range of 10–50 mV by keeping the frequency and step potential at 15 Hz and 6 mV, respectively (Fig. 4.9B). The peak current increased up to 35 mV and then it decreased. Thus, 35 mV was selected for optimum measurements (inset Fig. 4.9B). Finally, by taking the optimum values of amplitude at 35 mV and step potential at 6 mV, the effect frequency on current response was studied in the range of 10–25 Hz (Fig. 4.9C). The peak current for CAF and TP increased up to 20 Hz, but after 20 Hz the peak current decreased. As a result, the 20 Hz was selected as an optimal value for the subsequent determination (inset Fig. 4.9C).

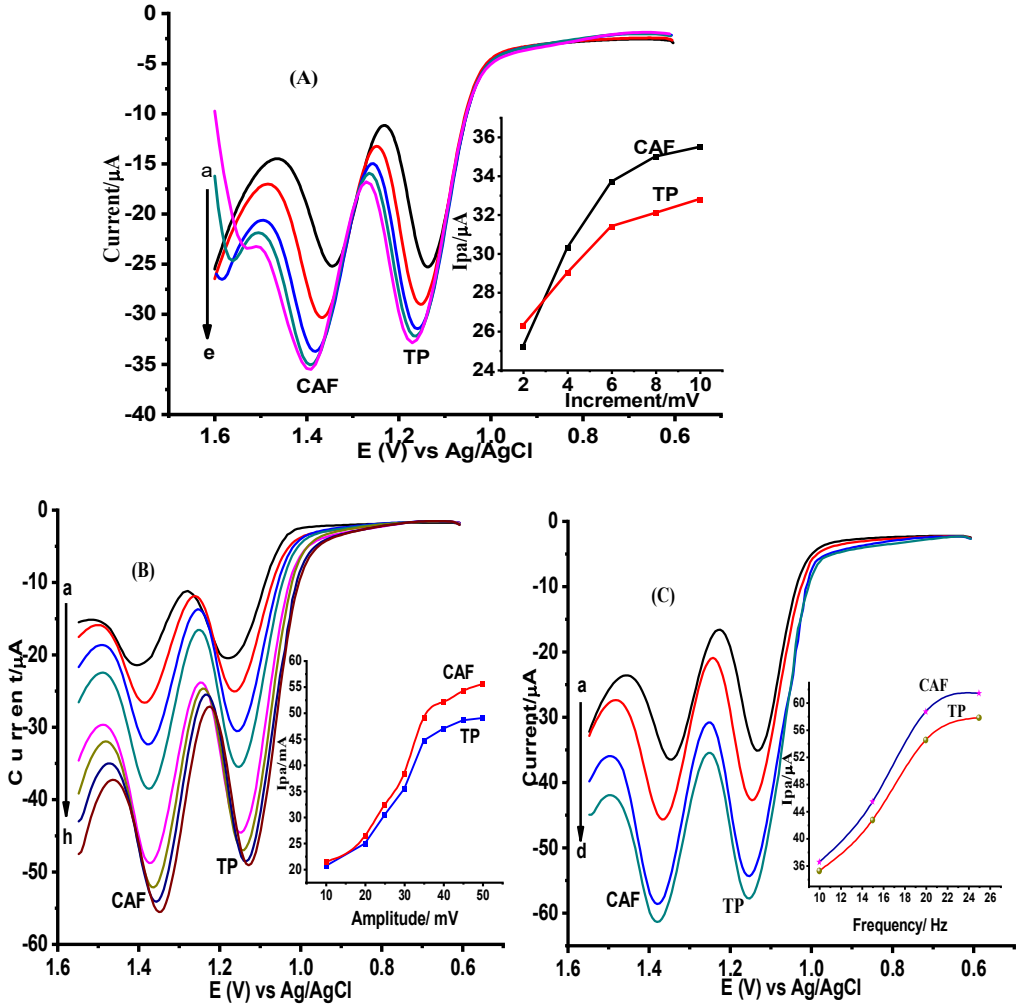

Figure 4.9: SWVs of poly(ACP_2CuIH)/GCE in pH 4.5 ABS containing 1.0 mM mixture of CAF and TP, (A) at various step potential (a–e: 2, 4, 6, 8, and 10 mV, respectively), amplitude of 25 mV, and frequency of 15 Hz. Inset: Plot of Ip vs. step potential, (B) at various square wave amplitudes (a–h: 10, 20, 25, 30, 35, 40, 45 and 50 mV, respectively), step potential of 6 mV, and frequency of 15 Hz. Inset: Plot of Ip vs. amplitude, (C) at step potential of 6 mV, amplitude of 35 mV, and various frequencies (a–d: 10, 15, 20, and 25 Hz, respectively). Inset: Plot of Ip vs. frequency.

4.4.2 Calibration Curves of TP and CAF

The dependence of square wave voltammetric current response of poly(ACP_2CuIH)/GCE on the concentration of TP and CAF were investigated. The study was conducted by varying the concentration of one while keeping the concentration of the other constant and even varying the concentration of both TP and CAF intending to evaluate the effect of one another. Figure

4.10A illustrates the SWV for different concentrations of CAF at fixed (60.0 µM) concentration of TP. While the current response for the constant concentration of TP is remained the same, the current response for CAF increased linearly with concentration in the range of 1–200.0 µM with regression equation and determination coefficient (R^2) Ipa/µA = -3.2 - 0.11C/µM, and 0.99946, respectively. Similarly, (Fig. 4.10B) the peak current of TP showed linear variation with its concentration in the range 1–200.0 µM at fixed 60.0 µM CAF with regression equation and determination coefficient (R^2) of Ipa/µA = -3.8 - 0.12C/µM, and 0.99865, respectively.

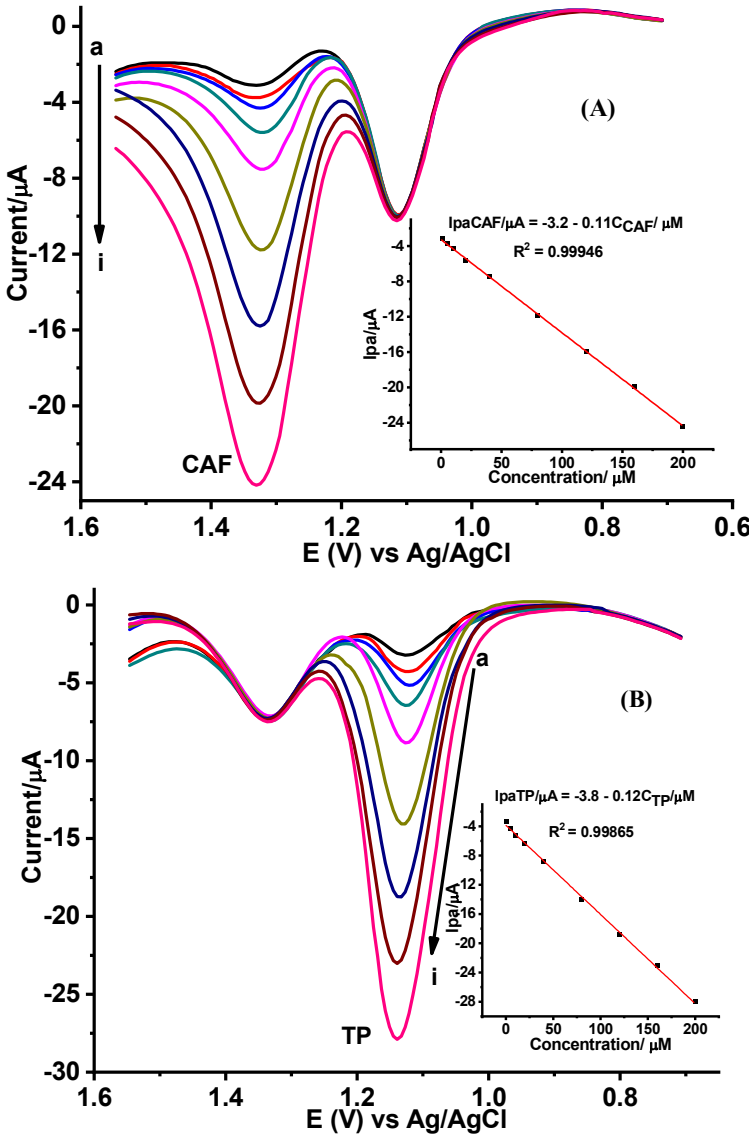

Figure 4.10: Background subtracted SWVs of poly (ACP_2CuIH)/GCE in pH 4.5 ABS containing different concentrations of (A) CAF (a–i: 1.0, 5.0, 10.0, 20.0, 40.0, 80.0, 120.0, 160.0, and 200.0 μM, respectively) and 60.0 μM TP, and (B) TP (a-i: 1.0, 5.0, 10.0, 20.0, 40.0, 80.0, 120.0, 160.0, and 200.0 μM, respectively) and 60.0 μM CAF. Insets: Plot of peak current vs. concentration, at step potential: 6 mV, amplitude: 35 mV, and frequency: 20 Hz.

The main objective of this study was to determine theophylline and caffeine simultaneously using poly(ACP_2CuIH)/GCE. Under the optimal experimental conditions, SWVs of simultaneously varying equi-molar concentrations of TP and CAF were recorded at poly(ACP_2CuIH)/GCE (Fig. 4.11A). Two well-shaped and separated peaks with increasing current magnitude as a function of concentration in the entire range of concentration were recorded. Surprisingly, the regression equations for the linear dependence of peak current on concentration for TP and CAF, even in the varying concentration mixture, showed exactly the same slope (Fig. 4.11B) as in the condition where one is kept constant showing that the surface of the electrode is not affected by products of analytes nor their concentration. The regression equations of TP; Ipa/μA = -3.2 - 0.11C/μM, and R^2 = 0.9990, and CAF; Ipa/μA = -3.8 - 0.12C/μM, and 0.9993, respectively.

The low associated %RSD values (below 3.62% for n = 3) of TP and (below 2.90% for n = 3) of CAF showed the accuracy and precision and hence validated the applicability of the developed method based on the poly(ACP_2CuIH)/GCE modified electrode for simultaneous determination of TP and CAF.

The detection limit was calculated by using the relationship (LoD = 3S/m) where S is the standard deviation of the blank measured under the same conditions as for the standard sample analysis (n = 6) and m is the slope of the calibration curve. The calculated method LoD of TP and CAF were 8.92×10^{-9} M and 1.02×10^{-8} M, respectively. The limit of quantification by using the relationship (LoQ = 10S/m) was also 3.4×10^{-8} M, and 2.97×10^{-8} M for TP and CAF, respectively.

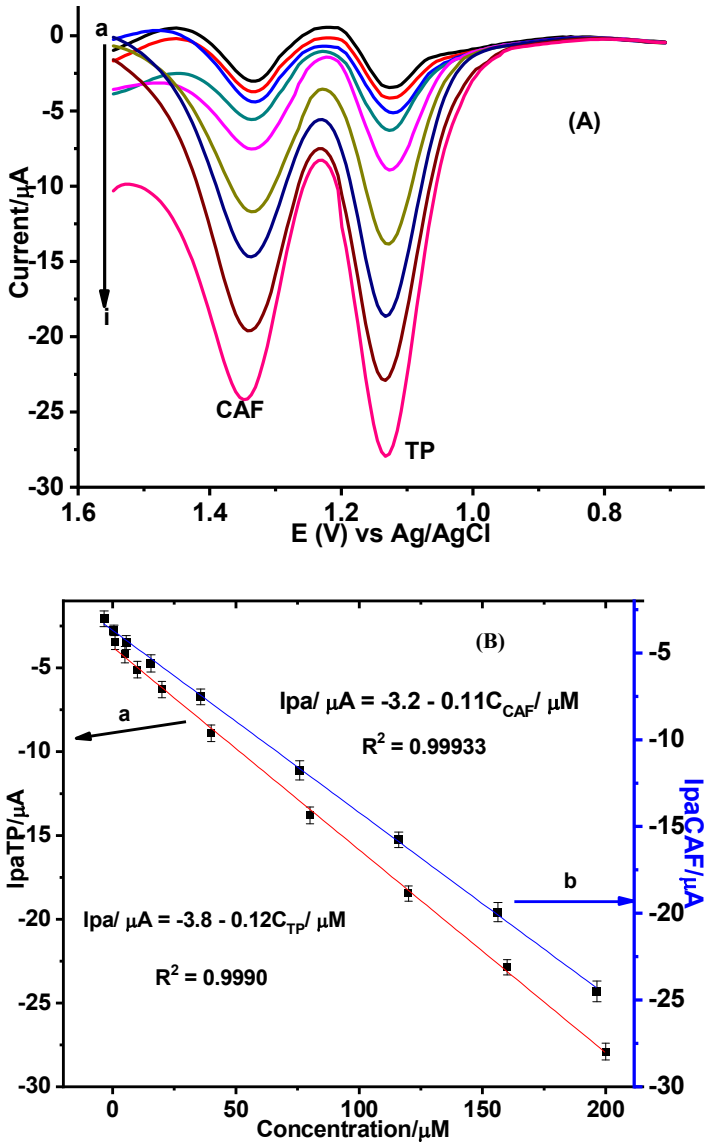

Figure 4.11: (A) Corrected for background SWVs of varying equi-molar mixtures of TP and CAF in pH 4.5 ABS (a–i: 1.0, 5.0, 10.0, 20.0, 40.0, 80.0, 120.0, 160.0 and 200.0 μM, respectively) at poly(ACP_2CuIH)/GCE. (B) Plot of the Ipa of TP (a) and CAF (b) (%RSD as error bar) vs. concentration, at step potential: 6 mV, amplitude: 35 mV, and frequency: 20 Hz.

4.5 Simultaneous Determination of CAF and TP in Real Samples

Under optimized solution pH and SWV parameters, the applicability of the developed method using poly(ACP_2CuIH)/GCE for simultaneous detection of CAF and TP in real samples, which may/may not contain both, was investigated. Three tea samples (Black-lion, Addis, and Wush wush), human blood serum, and pharmaceutical tablet formulation (Panadol extra, and theodrine) were used to see the practical applicability of the modified electrode in this study.

4.5.1 Tea Samples

The extract of each tea brand sample was first diluted with the supporting electrolyte as described under the experimental part and then determined concentrations of CAF and TP determined in tea samples. Among the two peaks obtained for all tea brands (Fig. 4.12), the one that appeared at the potential of standard CAF was assigned for CAF while the peak represented as "x" was ascribed for theobromine as reported in literature [69]. This confirmed the absence of detectable levels of TP in all analyzed tea samples. The detected caffeine levels in the analyzed tea samples in this study were 83.6 µg L^{-1} (Addis tea), 93.6 µg L^{-1} (Wush wush tea), and 98.2 µg L^{-1} (Black lion tea) (Fig. 4.12).

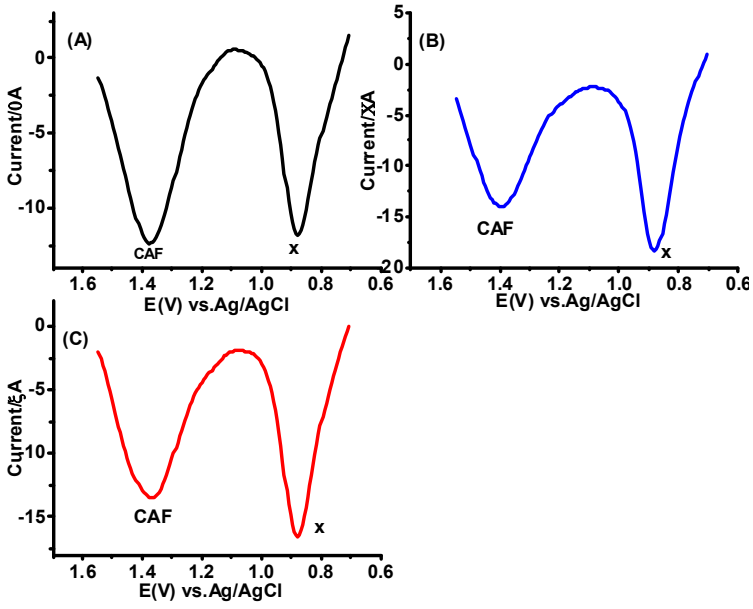

Figure 4.12: SWVs of poly(ACP_2CuIH)/GCE in pH 4.5 ABS containing (A) Addis tea, (B) Black lion tea, and (C) Wush wush tea at the optimized SWV parameters.

4.5.2 Tablet Samples

The developed SWV method using the polymer modified electrode was examined for its application for simultaneous detection of CAF and TP in two tablet types; Panadol extra known to contain caffeine, and Theodrine to contain TP. The CAF and TP content of the two analyzed tablet brands expressed as mg/tablet were determined and compared with the claimed value of panadol extra (65 mg/tablet CAF) and theodrine (120 mg/tablet TP) are summarized in Table 4.2. As can be seen from Fig. 4.13, while the voltammogram for the Panadol extra tablet showed only one peak assigned to CAF (Fig. 4.13A), the voltammogram for Theodrine also revealed only one peak assigned to TP (Fig. 4.13B). The detected CAF content in the Panadol extra tablet sample was 65.0 mg/tablet, and the TP content in the Theodrine 121.2 mg/tablet (Table 4.2).

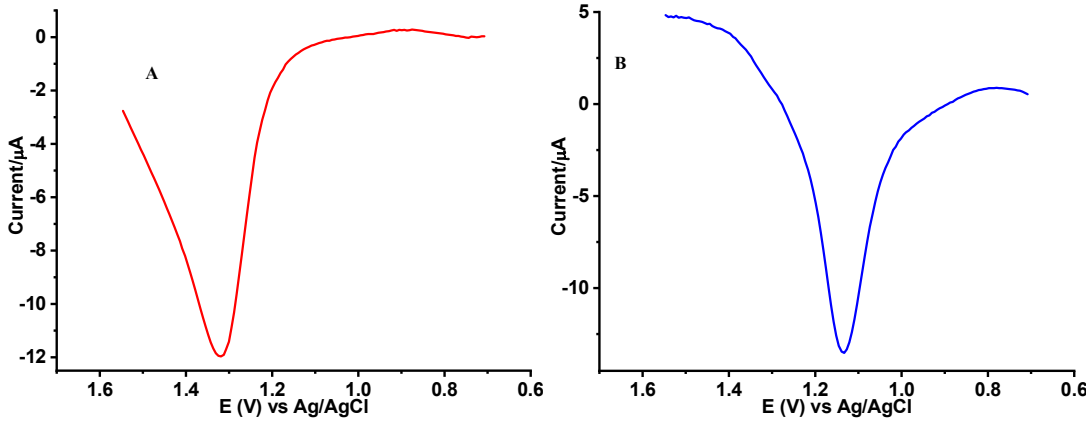

Figure 4.13: Corrected for blank SWVs of poly(ACP_2CuIH)/GCE in pH 4.5 PBS containing A) Panadol tablet brand, and B) Theodrine tablet brand at the optimized SWV parameters.

As can be seen from Table 4.2, the detected CAF and TP content in panadol extra and theodrine 100.0 and 101.0% of the companies' labels, respectively. In contrast to the expected level of CAF and TP in the two studied tablet brands, observed the accuracy and precision of the developed method and hence further validated the applicability of the method for determination of CAF and TP in a complex matrix.

Table 4.2 Summary of detected CAF and TP content in Panadol extra and Theodrine tablet samples using the developed method and percent detected as compared to the nominal value (n = 3).

Tablet	Expired date	Serial No.	Expected drug content (μM)	Detected drug in		Labeled value (mg/tablet)	Measured %
				Sample (μM)[a]	Tablet (mg/tablet)		
Panadol extra	11-2022	BN24129	80.0	80.0±1.5000	65.0	65 mg CAF	100.0
Theodrine	10-2022	Y056SP	80.0	80.8±1.8800	121.2	120 mg TP	101.0

[a] Detected mean tablet samples ± %RSD and data express for triplicate measurements.

4.5.3 Human Blood Serum Sample

The application of the proposed method was examined for the determination of both CAF and TP in human serum sample. The SWV for the unspiked human blood serum sample (curve a of Fig. 4.14) showed no peak in the scanned potential window indicating the absence of any oxidizable species including CAF and TP in its detectable level. To further validate the result, spike recovery analysis was conducted (section 4.6.1.1).

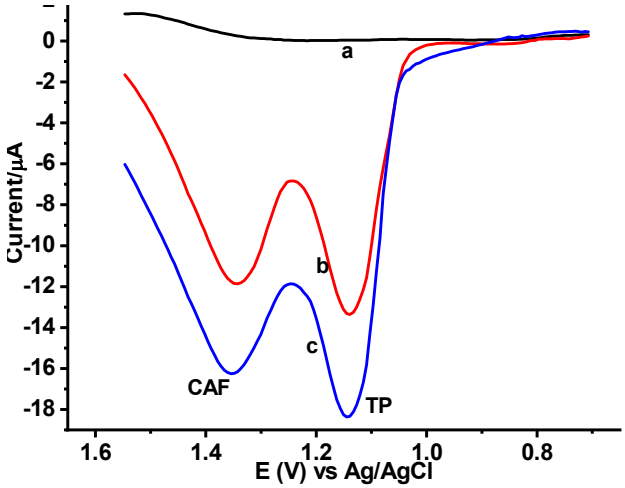

Figure 4.14: Corrected for blank SWVs of human blood serum in pH 4.5 ABS spiked with equi-molar mixtures of TP and CAF (a–c: 0.0, 80.0 μM mixture, and 120.0 μM mix of TP + CAF, respectively) at poly(ACP_2CuIH)/GCE.

4.6 Method Validation

The reliability of the results using the developed method was validated using selected validation parameters.

4.6.1 Spike Recovery Study

One of the validation parameters used was accuracy of the method which is checked by the spike recovery results.

4.6.1.1 Spike Recovery from Human Blood Serum Sample

The human blood serum samples spiked with 80.0 and 120.0 µM of both CAF and TP were analyzed for spike recovery analysis. While the unspiked serum sample showed no peak for both the CAF and TP, the spiked serum samples revealed two peaks; one for TP, and the other for CAF at the respective potentials (Fig. 4.14). The detected amounts of TP and CAF in the serum samples after spiked with 80.0 and 120.0 µM mixture of the two as calculated using the regression equation are summarized in Table 4.3. The recoveries of TP and CAF were obtained 100.0–101.4% and 98.9–99.3%, respectively, which indicates the practical applicability of the modified electrode for the simultaneous determination of TP and CAF in the clinical and biological samples.

Table 4.3 Simultaneous determination of TP and CAF in human blood serum samples spiked with an equi-molar mixture of TP and CAF standard (n= 3).

Sample	Analyte	Detected drug before spike (µM)	Spiked amount (µM)	Detected after spike (µM) [b]	Recovery (%)
Blood serum	TP	----------	120.0	121.7±0.0217	101.4
			80.0	80.0±0.0162	100.0
	CAF	----------	120.0	119.1±0.0268	99.3
			80.0	79.1±0.0243	98.9

[b] Detected mean serum samples ± %RSD and data express for triplicate.

4.6.1.2 Spike Recovery from Tea Samples

As discussed under the sample analysis section, the unspiked three tea brand samples all showed a peak for CAF and additional peak speculated to be theobromine (TB), but no peak for TP. Figure 4.15 presents SWVs for the unspiked and spiked tea samples (Black lion tea, Wush wush tea, and Addis tea) with various amounts of TP and CAF. As can be seen from

the (Fig. 4.15), while the peak intensity for TB remained constant in all the three tea samples, the peak intensity for CAF and TP also varied with the amount spiked. Remarkably, the voltammograms show almost the same signal intensity for equal amounts of each indicating the precision of the method.

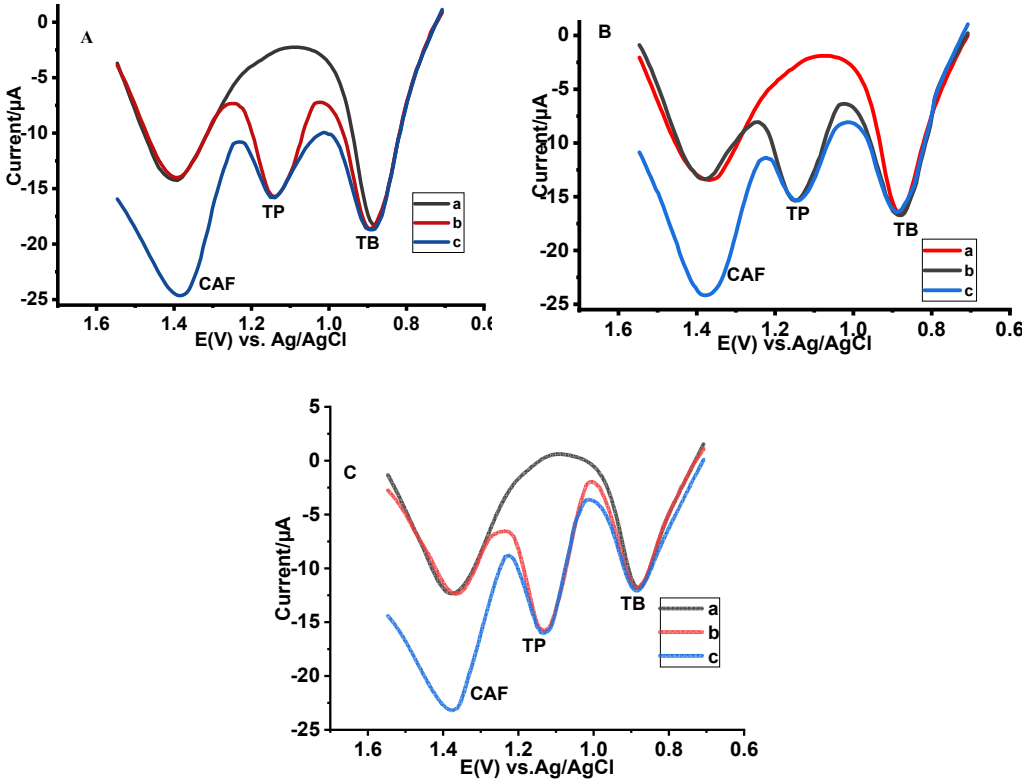

Figure 4.15: Corrected for blank SWVs of A) Black lion tea, B) Wush wush, and C) Addis tea samples all spiked with TP and CAF (a–c: real tea sample + 0.0 TP and CAF, a + 100.0 µM TP, and a + 100.0 µM + 100.0 µM CAF, respectively) at poly(ACP_2CuIH)/GCE.

The analyte level in each tea sample was calculated using the calibration regression equation. Spike recovery as a mean of triplicate measurements for TP and CAF in the three tea brand samples are summarized in Table 4.4. Spike recovery results in the range 97.0–102.0% for TP and 95.4–96.8% in tea samples showed the accuracy and hence validated the method for simultaneous determination of TP and CAF in real samples.

Table 4.4 Simultaneous determination of TP and CAF in Addis tea, Wush wush tea, and Black lion tea samples spiked with 100.0 µM TP and equi-molar mixture of 100.0 µM TP and CAF (n = 3).

Tea brand	Analyte	Detected (µM) [c]	Added (µM)	Found (µM) [d]	Recovery (%)
Addis	TP	----	100.0	100.0±0.0250	100.0
			100.0	102.0±0.0220	102.0
	CAF	83.6±1.3100	0	83.6±1.3100	--
			100.0	180.0±0.0158	96.4
Wush wush	TP	----	100.0	97.0±0.0223	97.0
			100.0	97.0±0.0216	97.0
	CAF	93.6±1.0700	0	93.6±1.0700	--
			100.0	189.0±0.0217	95.4
Black loin	TP	----	100.0	99.0±0.0318	99.0
			100.0	100.0±0.0315	100.0
	CAF	98.2±1.1700	0	98.2±1.1700	--
			100.0	195.0±0.0208	96.8

[c & d] Detected mean tea samples ± %RSD and data express for triplicate measurements.

4.6.1.3 Spike Recovery Study of Tablet Samples

Figure 4.16 presents SWVs for the two studied tablet brands spiked with TP and CAF. While the voltammogram for the unspiked Panadol extra tablet sample only shows a peak for CAF (curve a of Fig. 4.16 A), the Theodrine tablet shows a peak for TP (curve a of Fig. 4.16 B). As can be observed from the figure, the Panadol tablet spiked with both TP and CAF showed peak current increment on both analytes in proportion to the amount spiked. The same was also observed for the spiked Theodrine tablet sample. Spike recovery results of TP and CAF in tablet samples are summarized in Table 4.5. Excellent spike recovery results of TP and CAF in both tablet samples in the range 99.0–101.0 and 98.9–100.0, respectively further confirmed the accuracy of the developed method for its applicability for simultaneous determination of TP and CAF in real samples.

Table 4.5 Summary of spike recovery results (mean±%RSD, n = 3) of TP and CAF in Theodrine and Panadol extra tablet samples.

Tablet sample	Analyte	Initial detected(μM)	Added (μM)	Found (μM) [e]	Recovery (%)
Panadol extra	TP	-	80.0	79.2±0.0271	99.0
			80.0	79.2±0.0265	99.0
	CAF	80.0	0	80.0±1.5000	100.0
			80.0	159.1±0.0207	99.4
Theodrine	TP	80.0	0	80.8±1.8800	101.0
			80.0	160.0±0.0197	99.5
	CAF	-	80.0	79.1±0.0140	98.9
			80.0	79.1±0.0139	98.9

[e] Detected mean tablet samples ± %RSD and data express for triplicate.

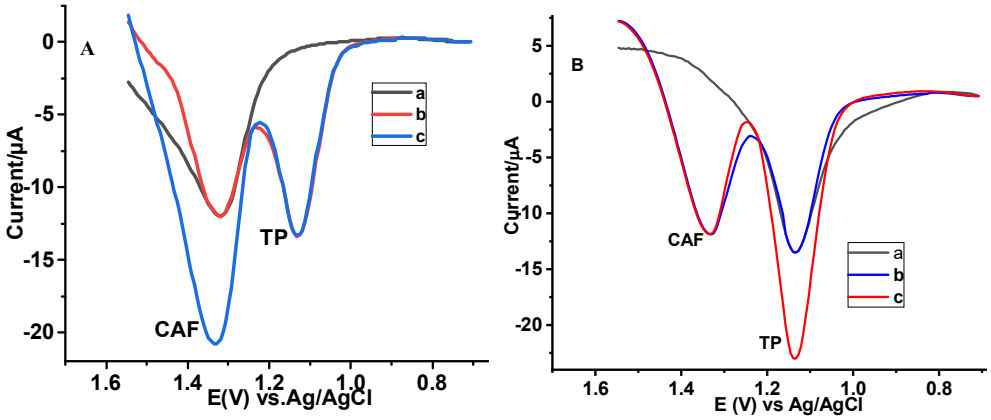

Figure 4.16: Corrected for blank SWVs of poly(ACP_2CuIH)/GCE in pH 4.5 ABS containing (A) Panadol tablet brand spiked with TP and CAF (a–c: unspiked tablet sample, a + 80.0 μM TP, and a + 80.0 μM each mix of TP and CAF, respectively), and (B) Theodrine tablet brand spiked with TP and CAF (a–c: unspiked tablet sample, a + 80.0 μM CAF, and a + 80.0 μM each mix of TP and CAF, respectively).

4.6.2 Interference Study

4.6.2.1 Interference Study of Tea Sample

The influence of various potentially interfering substances including urea, sodium chloride, paracetamol, and ephedrine at their various levels on the simultaneous determination of CAF and TP were investigated. To show the effect of the potential interferents on the simultaneous determination of TP and CAF in Black lion tea in this study, the tea sample was first spiked with a known amount of TP so that the sample can have both the TP and CAF. Figure 4.17

(A–D) present the SWVs of the Black lion tea samples spiked with potential interferents at their different levels (0–200.0 µM). As can be seen from the voltammograms, presence of any of the investigated four potential interferents did not cause the appearance of additional oxidative peak in the studied potential window.

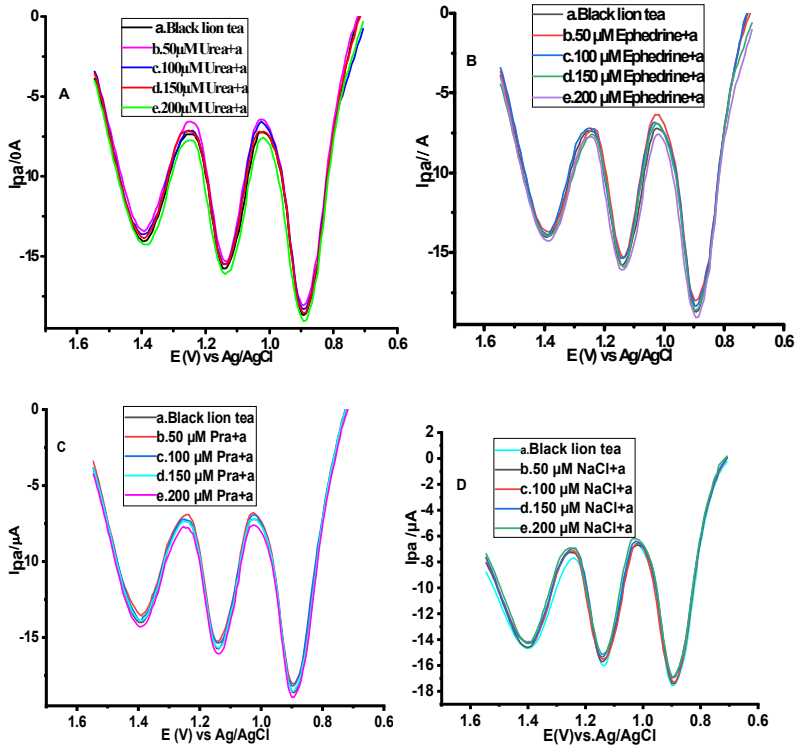

Figure 4.17: Corrected for blank SWVs of poly(ACP_2CuIH)/GCE in pH 4.5 ABS containing Black lion tea spiked with 100.0 µM TP in the presence of various concentrations (a–e: 0.0, 50.0, 100.0, 150.0, and 200.0 µM, respectively) of A) Urea, B) Ephedrine, C) Paracetamol, and D) Sodium chloride.

Percentage interference recovery results of TP and CAF in Black lion tea spiked with known amount of TP in the presence of potential interferents at various concentrations (0–200.0 µM) are summarized in Table 4.6. As can be seen from the table, the maximum concentration of thus foreign substances caused an approximately less than 5% relative error in the detection of TP and CAF (Fig. 4.17A–D). From the interference study, it seems that the proposed method is selective enough and can be applicable to the simultaneous detection of TP and CAF in tea samples. Moreover, the interference study suggests the possibility of the simultaneous determination of theophylline, caffeine, xanthine, and theobromine at the poly (ACP_2CuIH)/GCE modified electrode.

Table 4.6 Summary of percentage interference recovery results of TP and CAF in Black tea sample spiked with 100.0 µM TP in the presence of selected potential interferents (Urea, Paracetamol, Ephedrine, and Sodium chloride) at their various levels.

Interferent	Interferent added (µM)	Detected (µA)		Expected (µA)		Recovery (%)	
		TP	CAF	TP	CAF	TP	CAF
Urea	0	-15.7	-14.0	-15.8	-14.0	99.4	-
	50.0	-15.4	-13.4	-15.8	-14.0	97.5	95.7
	100.0	-15.5	-13.7	-15.8	-14.0	98.0	98.0
	150.0	-15.5	-13.9	-15.8	-14.0	98.0	99.0
	200.0	-16.0	-14.0	-15.8	-14.0	101.0	100.0
Sodium chloride	0	-15.7	-14.0	-15.8	-14.0	99.0	-
	50.0	-15.1	-14.0	-15.8	-14.0	96.0	100.0
	100.0	-15.3	-14.3	-15.8	-14.0	97.0	102.0
	150.0	-15.5	-14.3	-15.8	-14.0	98.1	102.0
	200.0	-15.9	-14.6	-15.8	-14.0	100.6	104.3
Paracetamol	0	-15.8	-14.0	-15.8	-14.0	100.0	-
	50.0	-15.3	-13.6	-15.8	-14.0	97.0	97.0
	100.0	-15.4	-13.9	-15.8	-14.0	98.0	99.0
	150.0	-15.7	-13.9	-15.8	-14.0	99.0	99.0
	200.0	-16.0	-14.0	-15.8	-14.0	101.0	100.0
Ephedrine	0	-15.8	-14.0	-15.8	-14.0	100	-
	50.0	-15.3	-13.7	-15.8	-14.0	97.0	98.0
	100.0	-15.4	-13.9	-15.8	-14.0	98.0	99.0
	150.0	-15.8	-13.9	-15.8	-14.0	100.0	99.0
	200.0	-16.0	-14.0	-15.8	-14.0	101.0	100.0

4.6.2.2 Interference Study of Tablet Sample

The influence of various potentially interfering substances including ascorbic acid (AA), glucose, ephedrine, and paracetamol on the simultaneous determination of TP and CAF in a mixture of tablet samples containing TP and CAF were investigated. Fig. 4.18 presents SWVs of the mixture of Panadol and Theodrine tablet samples with nominal concentrations of 80.0 µM TP and CAF in the presence of the potential interferents at their various levels. It is noted from the voltammograms that presence of any of the studied interferents did not cause the appearance of an oxidative peak in the studied potential range.

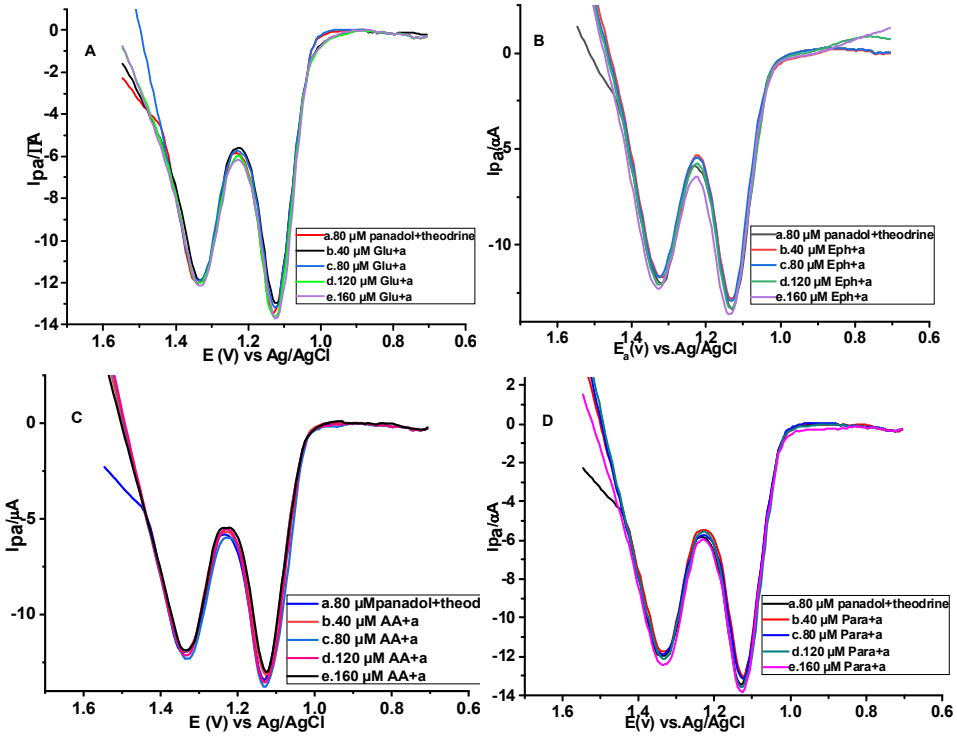

Figure 4.18: Corrected for blank SWVs of poly(ACP_2CuIH)/GCE in pH 4.5 ABS containing a mix of Panadol tablet with nominal 80.0 µmol L^{-1} CAF and Theodrine tablet with nominal 80.0 µmol L^{-1} TP in the presence of A) Glucose, B) Ephedrine, C) Ascorbic Acid, and D) Paracetamol of various concentrations (a-e: tablet mix + 0.0, a + 40.0, a + 80.0, a + 120.0, and a + 160.0 µmol L^{-1}, respectively).

The tolerance limit was taken as the maximum concentration of the foreign substances that caused an approximately ±3.7% relative error in the determination. The results (Table 4.7) show that 40.0, 80.0, 120.0 and 160.0 µM of glucose, paracetamol, ephedrine and ascorbic acid the present of 80.0 µM TP in Theodrine and 80.0 µM CAF in Panadol extra did not interfere in the simultaneous determination of TP and CAF (Figure 4.18 A–D). The SWV of blank Panadol extra tablet sample (Fig. 4.16A curve a) was shown only CAF and Theodrine tablet (Fig. 4.16B curve a) only TP oxidation peak the determination voltage range. This indicates the presence of other substances in Panadol extra tablet samples such as paracetamol and Theodrine such as ephedrine do not interfere with the simultaneous determination of TP and CAF. From the interference study, it seems that the proposed method is selective enough and can be applicable to the simultaneous detection of TP and CAF pharmaceutical tablet samples. Moreover, the interference study suggests the possibility

of the simultaneous determination of theophylline, caffeine, xanthine and theobromine at the poly(ACP_2CuIH) modified electrode.

Table 4.7 Summary of percentage interference recovery results of TP and CAF in tablet samples in the effect of potential interfering species on the simultaneous determination of 80.0 µM TP in Theodrine tablet and 80.0 µM CAF in Panadol extra tablet (n = 3)

Interferent	Interferent added (µM)	Detected (µA)		Expected (µA)		Recovery (%)	
		TP	CAF	TP	CAF	TP	CAF
Ascorbic acid	0	-13.5	-12.0	-13.5	-12.0		
	40.0	-13.1	-11.9	-13.5	-12.0	97.0	99.0
	80.0	-13.1	-11.9	-13.5	-12.0	97.0	99.0
	120.0	-13.5	-12.3	-13.5	-12.0	100.0	103.0
	160.0	-13.7	-12.0	-13.5	-12.0	101.0	100.0
Glucose	0	-13.5	-12.0	-13.5	-12.0		
	40.0	-13.0	-11.9	-13.5	-12.0	96.3	99.0
	80.0	-13.0	-11.9	-13.5	-12.0	96.3	99.0
	120.0	-13.5	-12.0	-13.5	-12.0	100.0	100.0
	160.0	-13.6	-12.0	-13.5	-12.0	100.7	100.0
Paracetamol	0	-13.5	-12.0	-13.5	-12.0		
	40.0	-13.1	-11.8	-13.5	-12.0	97.0	98.0
	80.0	-13.1	-11.9	-13.5	-12.0	97.0	99.0
	120.0	-13.5	-12.0	-13.5	-12.0	100.0	100.0
	160.0	-13.7	-12.4	-13.5	-12.0	101.0	103.0
Ephedrine	0	-13.5	-12.0	-13.5	-12.0		
	40.0	-13.0	-12.0	-13.5	-12.0	96.3	100.0
	80.0	-13.0	-11.7	-13.5	-12.0	96.3	98.0
	120.0	-13.3	-12.0	-13.5	-12.0	98.5	100.0
	160.0	-13.4	-12.0	-13.5	-12.0	99.3	100.0

4.7 Stability of the Poly(ACP_2CuIH)/GCE

The long-term stability was evaluated by keeping the electrode in pH 4.5 ABS for one day at room temperature. The peak current response of mixed 1.0 mM TP and CAF was measured every two hours for one day using SWV in pH 4.5 ABS. Figure 4.19 shows Five SWVs of the mixture at the polymer modified electrode recorded in a day at an interval of two hours. Detection of the analytes with a maximum associated error of 0.88% for TP and 1.1% for CAF indicates that the poly(ACP_2CuIH)/GCE modified electrode has excellent stability. In general, the precision, accuracy, selectivity, and stability of the new electrode modifier validated the developed method for determination of TP and CAF in real samples.

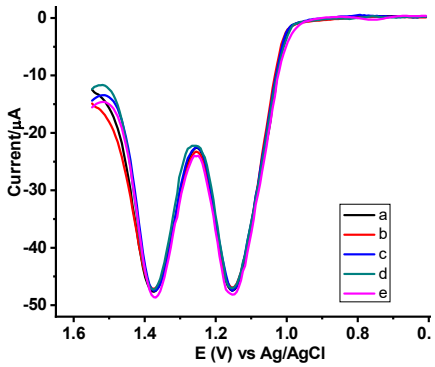

Figure 4.19: Five repetitive SWVs of poly(ACP_2CuIH)/GCE in pH 4.5 ABS containing a mixture of 1.0 M CAF and TP recorded in one day at an interval of two hrs.

4.8 Comparison of Present Method with Previously Reported Methods

A comparison between the analytical performance of the present method with methods in literature recently reported for simultaneous determination of TP and CAF was made. The results in Table 4.8 showed that the proposed method has a reasonably wide linear dynamic range and the lowest method LoD as compared to the selected literature values. Taking into account the simplicity of electrode surface modification, the observed wide linear dynamic range, and low method LoD, it is possible to conclude that the present method can be an excellent candidate for simultaneous determination of TP and CAF in real samples.

Table 4.8 Comparison of the performance of the present method with previously reported methods in terms of selected parameters.

Electrode type	Method	Analyte	Linear-range (µM)	LoD (µM)	Ref.
Poly(FA)/ GR /GCE	DPV	TP CAF	0.2–100 1.0–160	0.03 0.08	[17]
P(LAsp)/fMWCNT/GCE	SWV	TP CAF	0.1–50 1–150	0.020 0.28	[28]
P(L-Pal)/rGO/GCE	DPV	TP CAF	1–260 1–260	0.35 0.50	[32]
DP-PyCOF/AuNPs/GCE	DPV	TP CAF	0.9–20; 20–400 30–600	0.19 0.076	[39]
PLCYb/N-CNTc/GCE	DPV	TP CAF	1–70 0.4–140	0.033 0.02	[53]
Poly(ACP_2CuIH)/GCE	SWV	TP CAF	1–200 1–200	0.00892 0.0102	This work

5 CONCLUSION AND RECOMMENDATION

5.1 Conclusion

In this study, the application of poly(ACP_2CuIH)/GCE for simultaneous determination of CAF and TP in tea, human blood serum and tablet (Panadol extra and Theodrine) samples is reported for the first time. Cyclic voltammetry was employed for the study of the electrochemical behavior of CAF and TP, dependence of peak current on the scan rate, and pH of the solution. In contrast to the cyclic voltammetric response recorded for CAF and TP at unmodified GCE, appearance of well separated irreversible oxidation peak for both TP and CAF at reduced over potential with sufficient current enhancement at poly(ACP_2CuIH)/GCE signified excellent catalytic effect of the modifier towards CAF and TP. Under optimized solution, and SWV parameters, oxidative peak current response of the poly(ACP_2CuIH)/GCE showed linear dependence on the concentration of CAF and TP in the range 1.0 to 200.0 μM, with a R^2, and LoD (n = 6) of 0.9990 and 8.92×10^{-9} M for TP, and 0.9993 and 1.02×10^{-8} M for CAF. Furthermore, the method was successfully used for the quantification of TP and CAF in various samples including tea samples (Black lion, Addis, and Wush wush), pharmaceutical tablet samples (Panadol extra and Theodrine), and human blood serum real samples. Excellent spike recovery results TP and CAF in the range 97.0–102.0% and 95.4–96.8% in tea samples, 99.0–101.0, and 98.9–100.0, in tablet samples, and 100.0–101.4% and 98.9–99.3%, in human blood serum samples, respectively. Wide dynamic concentration range, high precision, extremely low detection limit, excellent recovery results, and high recovery results even in the presence of selected potential interference validated the applicability of the developed method for simultaneous determination of CAF and TP in real samples, making the method an excellent potential candidate. In general, the proposed method provides a useful tool for the simultaneous determination of TP and CAF in food, biological, pharmaceutical tablet analysis, and clinical sample applications.

5.2 Recommendation

It is recommended that further investigations are required for determination of CAF and TP in other pharmaceutical tablets, food, and clinical samples at the poly(ACP_2CuIH)/GCE modified electrode and the reproducibility of the electrode also ought to be conducted. The surface characterization of the modified electrode should be also conducted by using FTIR, SEM, XRD, and UV. The results obtained in this method using poly(ACP_2CuIH)/GCE modified GCE are better to be compared with other conventional methods and also interferences other than glucose, urea, sodium chloride, paracetamol, ephedrine, and ascorbic acid are better to be studied using the same electrode.

6 REFERENCES

[1] Suravajhala, R., N. Suri, M. Bhagat, and A. Saxena, Biological evaluation of 8-alkyl xanthines as potential cytotoxic agents. Advances in Biological Chemistry, 2013. 3:314-319 https://doi:10.4236/abc.2013.33035.

[2] Lo Coco, F., F. Lanuzza, G. Micali, and G. Cappellano, Determination of theobromine, theophylline, and caffeine in by-products of cupuacu and cacao seeds by high-performance liquid chromatography. Journal of Chromatographic Science, 2007. 45(5):273-275 https://doi:10.1093/chromsci/45.5.273.

[3] Srdjenovic, B., V. Djordjevic-Milic, N. Grujic, R. Injac, and Z. Lepojevic, Simultaneous HPLC determination of caffeine, theobromine, and theophylline in food, drinks, and herbal products. Journal of Chromatographic Science, 2008. 46(2):144-149 https://doi.org/10.1093/chromsci/46.2.144.

[4] Chen, Q.-c., S.-f. Mou, X.-p. Hou, and Z.-m. Ni, Simultaneous determination of caffeine, theobromine and theophylline in foods and pharmaceutical preparations by using ion chromatography. Analytica Chimica Acta, 1998. 371(2):287-296 https://doi.org/10.1016/S0003-2670(98)00301-8.

[5] Weldegebreal, B., M. Redi-Abshiro, and B.S. Chandravanshi, Development of new analytical methods for the determination of caffeine content in aqueous solution of green coffee beans. Chemistry Central Journal, 2017. 11(1):1-9 https://doi.org/10.1186/s13065-017-0356-3.

[6] Filik, H., A.A. Avan, and Y. Mümin, Simultaneous electrochemical determination of caffeine and vanillin by using poly(Alizarin Red S) modified glassy carbon electrode. Food Analytical Methods, 2017. 10(1):31-40 http://doi/10.1007/s12161-016-0545-z

[7] Turnbull, D., J.V. Rodricks, G.F. Mariano, and F. Chowdhury, Caffeine and cardiovascular health. Regulatory Toxicology and Pharmacology, 2017. 89:165-185 https://doi.org/10.1016/j.yrtph.2017.07.025.

[8] Nawrot, P., S. Jordan, J. Eastwood, J. Rotstein, A. Hugenholtz, and M. Feeley, Effects of caffeine on human health. Food Additives and Contaminants, 2003. 20(1):1-30 https://doi:10.1080/0265203021000007840.

[9] Chapman, R. and T. Mickleborough, The effects of caffeine on ventilation and pulmonary function during exercise: An often-overlooked response. The Physician and Sportsmedicine, 2009. 37:97-103 https://doi.org/10.3810/psm.2009.12.1747.

[10] Llobat-Estelles, M., R. Marin-Saez, and M.S.-M. Ciges, Spectrophotometric determination of the theophylline in plasma by the apparent content curves method. Talanta, 1996. 43(9):1589-1594 https://doi.org/10.1016/0039-9140(96)01902-9.

[11] Li, H., M. Roxo, X. Cheng, S. Zhang, H. Cheng, and M. Wink, Pro-oxidant and lifespan extension effects of caffeine and related methylxanthines in Caenorhabditis elegans. Food Chemistry: X, 2019. 1:1-9 https://doi.org/10.1016/j.fochx.2019.100005.

[12] Huck, C., W. Guggenbichler, and G. Bonn, Analysis of caffeine, theobromine and theophylline in coffee by near infrared spectroscopy (NIRS) compared to high-performance liquid chromatography (HPLC) coupled to mass spectrometry. Analytica Chimica Acta, 2005. 538(1-2):195-203 https://doi.org/10.1016/j.aca.2005.01.064.

[13] Sereshti, H., M. Khosraviani, S. Samadi, and M.S. Amini-Fazl, Simultaneous determination of theophylline, theobromine and caffeine in different tea beverages by graphene-oxide based ultrasonic-assisted dispersive micro solid-phase extraction combined with HPLC-UV. RSC Advances, 2014. 4(87):47114-47120 https://doi.org/10.1039/C4RA06412G.

[14] Jafari, M., B. Rezaei, and M. Javaheri, A new method based on electrospray ionisation ion mobility spectrometry (ESI-IMS) for simultaneous determination of caffeine and theophylline. Food Chemistry, 2011. 126(4):1964-1970 https://doi.org/10.1016/j.foodchem.2010.12.054.
[15] Zhu, T. and K.H. Row, Simultaneous determination of caffeine and theophylline in human plasma with a weak cation monolithic SPE-column. Chinese Journal of Chemistry, 2010. 28(8):1463-1468 https://doi.org/10.1002/cjoc.201090250.
[16] Singh, D. and A. Sahu, Spectrophotometric determination of caffeine and theophylline in pure alkaloids and its application in pharmaceutical formulations. Analytical Biochemistry, 2006. 349(2):176-180 https://doi.org/10.1016/j.ab.2005.03.007.
[17] Shu, X., F. Bian, Q. Wang, X. Qin, and Y. Wang, Electrochemical sensor for simultaneous determination of theophylline and caffeine based on a novel poly (folic acid)/graphene composite film modified electrode. International Journal of Electrochemical Science, 2017. 12:4251-4264 https://doi:10.20964/2017.05.37.
[18] Amare, M. and S. Admassie, Differential pulse voltammetric determination of theophylline at poly (4-amino-3-hydroxyl naphthalene sulfonic acid) modified glassy carbon electrode. Bulletin of the Chemical Society of Ethiopia, 2012. 26(1):73-84 https://dx.doi.org/10.4314/bcse.v26i1.8.
[19] Monteiro, M.K.S., D.R. Da Silva, M.A. Quiroz, V.J.P. Vilar, C.A. Martínez-Huitle, and E.V. Dos Santos, Applicability of cork as novel modifiers to develop electrochemical sensor for caffeine determination. Materials, 2021. 14(1):1-17 https://doi.org/10.3390/ma14010037
[20] Qiao, J., L. Zhang, S. Gao, and N. Li, Facile fabrication of graphene-supported Pt electrochemical sensor for determination of caffeine. Applied Biochemistry and Biotechnology, 2020. 190(2):529-539 https://doi.org/10.1007/s12010-019-03104-z.
[21] Masibi, K.K., O.E. Fayemi, A.S. Adekunle, E.S.M. Sherif, and E.E. Ebenso, Electrochemical Determination of Caffeine Using Bimetallic Au−Ag Nanoparticles Obtained from Low-cost Green Synthesis. Electroanalysis, 2020. 32(12):2745-2755 https://doi.org/10.1002/elan.202060198.
[22] Killedar, L.S., M.M. Shanbhag, N.P. Shetti, S.J. Malode, R.S. Veerapur, and K.R. Reddy, Novel graphene-nanoclay hybrid electrodes for electrochemical determination of theophylline. Microchemical Journal, 2021. 165:106115 https://doi.org/10.1016/j.microc.2021.106115.
[23] Iranmanesh, T., S. Jahani, M.M. Foroughi, M.S. Zandi, and H.H. Nadiki, Synthesis of La_2O_3/MWCNT nanocomposite as the sensing element for electrochemical determination of theophylline. Analytical Methods, 2020. 12(35):4319-4326 https://doi.org/10.1039/D0AY01336F.
[24] Cinková, K., N. Zbojeková, M. Vojs, M. Marton, A. Samphao, and Ľ. Švorc, Electroanalytical application of a boron-doped diamond electrode for sensitive voltammetric determination of theophylline in pharmaceutical dosages and human urine. Analytical Methods, 2015. 7(16):6755-6763 https://doi.org/10.1039/C5AY01493J.
[25] Gao, Y., H. Wang, and L. Guo, Simultaneous determination of theophylline and caffeine by large mesoporous carbon/Nafion modified electrode. Journal of Electroanalytical Chemistry, 2013. 706:7-12 https://doi.org/10.1016/j.jelechem.2013.07.030.

[26] Jesny, S. and K. Girish Kumar, Non-enzymatic electrochemical sensor for the simultaneous determination of xanthine, its methyl derivatives theophylline and caffeine as well as its metabolite uric acid. Electroanalysis, 2017. 29(7):1828-1837 https://doi.org/10.1002/elan.201700115.
[27] Wang, Y., T. Wu, and C.-y. Bi, Simultaneous determination of acetaminophen, theophylline and caffeine using a glassy carbon disk electrode modified with a composite consisting of poly (Alizarin Violet 3B), multiwalled carbon nanotubes and graphene. Microchimica Acta, 2016. 183(2):731-739 https://doi:10.1007/s00604-015-1688-0.
[28] Mekassa, B., M. Tessema, and B.S. Chandravanshi, Simultaneous determination of caffeine and theophylline using square wave voltammetry at poly (L-aspartic acid)/functionalized multi-walled carbon nanotubes composite modified electrode. Sensing and Bio-sensing Research, 2017. 16:46-54 https://doi.org/10.1016/j.sbsr.2017.11.002.
[29] Kassa, A., A. Abebe, and M. Amare, Synthesis, characterization, and electropolymerization of a novel Cu (II) complex based on 1, 10-phenanthroline for electrochemical determination of amoxicillin in pharmaceutical tablet formulations. Electrochimica Acta, 2021:1-15 https://doi.org/10.1016/j.electacta.2021.138402.
[30] Favrod-Coune, T. and B. Broers, Addiction to caffeine and other xanthines, in Textbook of Addiction Treatment. 2021, Springer215-228 https://doi:10.1007/978-3-030-36391-8_16.
[31] Ejuh, G.W., J.M.B. Ndjaka, F. Tchangnwa Nya, P.L. Ndukum, C. Fonkem, Y. Tadjouteu Assatse, and R.A. Yossa Kamsi, Determination of the structural, electronic, optoelectronic and thermodynamic properties of the methylxanthine molecules theophylline and theobromine. Optical and Quantum Electronics, 2020. 52(11):1-22 (https://doi.org/10.1007/s11082-020-02617-w)
[32] Zhang, L., T. Wang, X. Fan, D. Deng, Y. Li, X. Yan, and L. Luo, Simultaneous determination of theophylline and caffeine using poly(L-phenylalanine)-reduced graphene oxide modified glassy carbon electrode. International Journal of Electrochemical Science, 2021. 16(4):1-11 https://doi:10.20964/2021.04.22.
[33] Amare, M. and S. Admassie, Polymer modified glassy carbon electrode for the electrochemical determination of caffeine in coffee. Talanta, 2012. 93:122-128 https://doi.org/10.1016/j.talanta.2012.01.058.
[34] Arnaud, M., The pharmacology of caffeine, in Progress in drug research/Fortschritte der Arzneimittelforschung/Progrès des recherches pharmaceutiques. 1987, Springer273-313 https://doi.org/10.1007/978-3-0348-9289-6_9.
[35] Manikandan, V.S., B. Adhikari, and A. Chen, Nanomaterial based electrochemical sensors for the safety and quality control of food and beverages. Analyst, 2018. 143(19):4537-4554 https://doi.org/10.1039/C8AN00497H.
[36] Ehlers, A., G. Marakis, A. Lampen, and K.I. Hirsch-Ernst, Risk assessment of energy drinks with focus on cardiovascular parameters and energy drink consumption in Europe. Food and Chemical Toxicology, 2019. 130:109-121 https://doi.org/10.1016/j.fct.2019.05.028.
[37] Barnes, P.J., Theophylline. American journal of respiratory and critical care medicine, 2013. 188(8):901-906 https://doi.org/10.1164/rccm.201302-0388PP
[38] Goodman, L.S., Goodman and Gilman's the pharmacological basis of therapeutics. Vol. 1549. 1996: McGraw-Hill New York.

[39] Guan, Q., H. Guo, R. Xue, M. Wang, N. Wu, Y. Cao, X. Zhao, and W. Yang, Electrochemical sensing platform based on covalent organic framework materials and gold nanoparticles for high sensitivity determination of theophylline and caffeine. Microchimica Acta, 2021. 188(3):1-11 https://doi:10.1007/s00604-021-04744-x.
[40] Uslu, B. and S.A. Ozkan, Electroanalytical methods for the determination of pharmaceuticals: a review of recent trends and developments. Analytical Letters, 2011. 44(16):2644-2702 https://doi.org/10.1080/00032719.2011.553010.
[41] Alemayehu, D., B.S.C. Chandravanshi, T. Hailu, and M. Tessema, Square wave anodic stripping voltammetric determination of Hg (II) with Np-chlorophenylcinnamohydroxamic acid modified carbon paste electrode. Bulletin of the Chemical Society of Ethiopia, 2020. 34(1):25-39 https://dx.doi.org/10.4314/bcse.v34i1.3.
[42] Kounaves, S.P., Voltammetric techniques. 1997, Prentice Hall, Upper Saddle River, NJ, USA709-726.
[43] Farghaly, O., R.A. Hameed, and A.-A.H. Abu-Nawwas, Electrochemical analysis techniques: a review on recent pharmaceutical applications. International Journal of Pharmaceutical Sciences Review and Research, 2014. 25:37-45.
[44] Ozkan, S.A., J.-M. Kauffmann, and P. Zuman, Electroanalytical techniques most frequently used in drug analysis, in Electroanalysis in biomedical and pharmaceutical sciences. 2015, Springer45-81 https://doi:10.1007/978-3-662-47138-8_3.
[45] Wang, J., Analytical Electrochemistry, VCH, Publishers. Inc., New York, 1994.
[46] Farghaly, O.A., R.A. Hameed, and A.-A.H. Abu-Nawwas, Analytical application using modern electrochemical techniques. International Journal of Electrochemical Science, 2014. 9(1):3287-3318.
[47] Bard, A.J. and L.R. Faulkner, Fundamentals and applications. Electrochemical Methods, 2001. 2(482):580-632.
[48] Zoski, C.G., Handbook of electrochemistry. 2006: Elsevier.
[49] Gosser, D.K., Cyclic voltammetry: simulation and analysis of reaction mechanisms. Vol. 43. 1993: VCH New York http://dx.doi.org/10.1080/00945719408001398.
[50] Barker, G.C. and A.W. Gardner, Pulse polarography. Fresenius' Zeitschrift für analytische Chemie, 1960. 173(1):79-83 Barker, G.C. and A.W. Gardner, Pulse polarography. Fresenius' Zeitschrift für analytische Chemie, 1960. 173(1):79-83 https://doi.org/10.1007/BF00448718.
[51] Barón-Jaimez, J., M. Joya, and J. Barba-Ortega. Anodic stripping voltammetry–ASV for determination of heavy metals. in Journal of Physics: Conference Series. 2013.IOP Publishing (https://iopscience.iop.org/1742-6596/466/1/012023).
[52] Osteryoung, J.G. and M.M. Schreiner, Recent advances in pulse voltammetry. CRC Critical Reviews in Analytical Chemistry, 1988. 19(sup1):S1-S27 https://doi.org/10.1080/15476510.1988.10401465.
[53] Wang, Y., Y. Ding, L. Li, and P. Hu, Nitrogen-doped carbon nanotubes decorated poly (L-Cysteine) as a novel, ultrasensitive electrochemical sensor for simultaneous determination of theophylline and caffeine. Talanta, 2018. 178:449-457 https://doi.org/10.1016/j.talanta.2017.08.076.
[54] Osteryoung, J.G. and R.A. Osteryoung, Square wave voltammetry. Analytical Chemistry, 1985. 57(1):101-110 https://doi.org/10.1021/ac00279a004.
[55] Mirceski, V., S. Komorsky-Lovric, and M. Lovric, Square-wave voltammetry: theory and application. 2007: Springer Science & Business Media.

[56] Lovrić, M., Square-wave voltammetry, in Electroanalytical methods. 2010, Springer121-145 https://doi:10.1007/978-3-642-02915-8_6
[57] Borman, S., New electroanalytical pulse techniques. Analytical Chemistry, 1982. 54(6):A698-A705 https://doi.org/10.1021/ac00243a728.
[58] Ozkan, S.A., J.-M. Kauffmann, and P. Zuman, Electroanalytical techniques most frequently used in drug analysis. Electroanalysis in Biomedical and Pharmaceutical Sciences, 2015:45-81 https://link.springer.com/chapter/10.1007/978-3-662-47138-8_3.
[59] Kokkinos, C., I. Raptis, A. Economou, and T. Speliotis, Disposable micro-fabricated electrochemical bismuth sensors for the determination of Tl (I) by stripping voltammetry. Procedia Chemistry, 2009. 1(1):1039-1042 https://doi.org/10.1016/j.proche.2009.07.259.
[60] Guadalupe, A.R. and H.D. Abruna, Electroanalysis with chemically modified electrodes. Analytical Chemistry, 1985. 57(1):142-149 https://pubs.acs.org/doi/10.1021/ac00279a036.
[61] Wang, J. and T. Martinez, Trace analysis at clay-modified carbon paste electrodes. Electroanalysis, 1989. 1(2):167-172 https://doi.org/10.1002/elan.1140010213.
[62] He, B. and S. Yan, Electrochemical determination of sulfonamide based on glassy carbon electrode modified by Fe3O4/functionalized graphene. International Journal of Electrochemical Science 2017. 12:3001-3011 https://doi:10.20964/2017.04.56.
[63] Kassa, A., M. Amare, and R.M. Mahfouz, Electrochemical determination of paracetamol, rutin and sulfonamide in pharmaceutical formulations by using glassy carbon electrode – A Review. Cogent Chemistry, 2019. 5(1):1-11 https://doi.org/10.1080/23312009.2019.1681607.
[64] Ensafi, A.A. and H. Karimi-Maleh, Modified multiwall carbon nanotubes paste electrode as a sensor for simultaneous determination of 6-thioguanine and folic acid using ferrocenedicarboxylic acid as a mediator. Journal of Electroanalytical Chemistry, 2010. 640(1-2):75-83 https://doi.org/10.1016/j.jelechem.2010.01.010.
[65] Moghaddam, A.B., A. Mohammadi, and M. Fathabadi, Application of carbon nanotube-graphite mixture for the determination of diclofenac sodium in pharmaceutical and biological samples. Pharmaceutica Analytica Acta, 2012. 3:1-6 https://doi:10.4172/2153-2435.1000161.
[66] Sun, J.-Y., K.-J. Huang, S.-Y. Wei, and Z.-W. Wu, Application of cetyltrimethylammonium bromide–graphene modified electrode for sensitive determination of caffeine. Canadian Journal of Chemistry, 2011. 89(6):697-702 https://doi.org/10.1139/v11-060.
[67] Sun, J.-Y., K.-J. Huang, S.-Y. Wei, Z.-W. Wu, and F.-P. Ren, A graphene-based electrochemical sensor for sensitive determination of caffeine. Colloids and Surfaces B: Biointerfaces, 2011. 84(2):421-426 https://doi.org/10.1016/j.colsurfb.2011.01.036.
[68] Daneshgar, P., P. Norouzi, M.R. Ganjali, A. Ordikhani-Seyedlar, and H. Eshraghi, A dysprosium nanowire modified carbon paste electrode for determination of levodopa using fast Fourier transformation square-wave voltammetry method. Colloids and surfaces. B, Biointerfaces, 2009. 68(1):27-32 https://doi.org/10.1016/j.colsurfb.2008.09.019.
[69] Nia, N.A., M.M. Foroughi, and S. Jahani, Simultaneous determination of theobromine, theophylline, and caffeine using a modified electrode with petal-like MnO_2 nanostructure. Talanta, 2021. 222:1-12 https://doi.org/10.1016/j.talanta.2020.121563.